

Diffusion magnetic resonance imaging in preterm brain injury

Anand S. Pandit · Gareth Ball · A. David Edwards ·
Serena J. Counsell

Received: 17 June 2013 / Accepted: 9 July 2013 / Published online: 14 August 2013
© Springer-Verlag Berlin Heidelberg 2013

Abstract

Introduction White matter injury and abnormal maturation are thought to be major contributors to the neurodevelopmental disabilities observed in children and adolescents who were born preterm. Early detection of abnormal white matter maturation is important in the design of preventive, protective, and rehabilitative strategies for the management of the preterm infant. Diffusion-weighted magnetic resonance imaging (d-MRI) has become a valuable tool in assessing white matter maturation and injury in survivors of preterm birth. In this review, we aim to (1) describe the basic concepts of d-MRI; (2) evaluate the methods that are currently used to analyse d-MRI; (3) discuss neuroimaging correlates of preterm brain injury observed at term corrected age; during infancy, adolescence and in early adulthood; and (4) explore the relationship between d-MRI measures and subsequent neurodevelopmental performance.

Methods References for this review were identified through searches of PubMed and Google Scholar before March 2013.

Results The impact of premature birth on cerebral white matter can be observed from term-equivalent age through to adulthood. Disruptions to white matter development, identified by d-MRI, are related to diminished performance in functional domains including motor performance, cognition and behaviour in early childhood and in later life.

Conclusion d-MRI is an effective tool for investigating preterm white matter injury. With advances in image acquisition and analysis approaches, d-MRI has the potential to be a

biomarker of subsequent outcome and to evaluate efficacy of clinical interventions in this population.

Keywords Preterm · Brain · Diffusion magnetic resonance imaging

Introduction

Preterm birth constitutes a major public health concern. With more than one in ten babies in the USA now being born preterm, the incidence is high and projected to increase (WHO 2012). The healthcare and societal burden attributed to the associated mortality and morbidity is considerable [1]. Financial costs including medical treatment, days spent in hospital, long-term care and specialist education are estimated annually at £3 billion in the UK [2] and \$26.2 billion in the USA [3]. In addition, there are profound negative emotional and psychosocial effects on both the individual and the supporting family [4].

Due to advances in neonatal care, mortality after preterm birth has decreased. However, preterm survivors are at risk of several adverse outcomes including neurodevelopmental impairments [4]. These include severe disabilities such as developmental delay, cerebral palsy (CP) and sensory impairments but also milder, persistent neurological deficits. Infants born premature have, on average, a 12-point reduction in IQ [5], reduced linguistic and motor abilities [6, 7], poor attention and social skills [8] and a reduced likelihood of completing higher education [9]. These latter problems can occur in the absence of severe disability and are inversely associated with gestational age at birth, with extremely premature infants being the most afflicted.

Pathogenesis of white matter injury

Cerebral white matter injury (WMI) is common after preterm birth and may underly the neurological impairments observed

This article is part of the special supplement “The Premature Brain”—Guest Editor: Charles Raybaud

A. S. Pandit · G. Ball · A. D. Edwards · S. J. Counsell (✉)
Centre for the Developing Brain, Department of Perinatal Imaging,
Division of Imaging Sciences and Biomedical Engineering, King’s
College London, First Floor, South Wing, St Thomas’ Hospital,
London SE1 7EH, UK
e-mail: serena.counsell@kcl.ac.uk

in this population [10]. Periventricular leukomalacia (PVL) typically consists of focal, cystic necrotic lesions surrounded by diffuse abnormalities and represents a severe manifestation of WMI. Cystic PVL is associated with serious disabilities such as CP but is relatively uncommon, affecting less than 5 % of preterm infants. In contrast, diffuse and focal, non-cystic changes are prevalent in the preterm population [11] and are likely to explain the more extensively observed, mild to moderate neurological deficits. Whilst focal lesions have relatively precise imaging correlates, diffuse WMI is more difficult to identify using conventional neuroimaging techniques. Fortunately, diffusion-weighted magnetic resonance imaging (d-MRI) shows greater sensitivity to these subtle changes and has become the tool of choice to study white matter (WM) microstructure in the preterm brain (see later).

The next section offers a concise summary of the key pathological events underlying preterm WMI. For reviews on this subject, we refer the reader to [12, 13]. Perinatal hypoxia–ischemia and/or infection can initiate a destructive cascade [14, 15], which results in exposure to excitotoxicity [16], oxidative stress [17] and inflammation [18, 19]. These processes take place in a developmentally sensitive window that would normally span the late second and third trimester. In this gestational period, the brain is vulnerable to these destructive influences. The fetal cerebrovascular system is particularly underdeveloped. Preterm neonates possess a poorly developed cerebral circulation [20], with low WM vascularity [21] and some evidence suggest that it is pressure-passive [22] with impaired auto-regulation [23]. In addition, preterm neonates are at risk of hypocarbia with attendant reductions in cerebral perfusion [24] and hyperoxia, due to the withdrawal of physiological hypoxia existing in utero, which can affect neurogenesis [25].

Some important cell populations are vulnerable to these deleterious influences. Premyelinating oligodendrocytes (preOLs), subplate neurons and late migrating GABAergic neurons show a heightened susceptibility to mediators of pathogenicity, namely, extracellular glutamate [16, 26], free radicals [17] and proinflammatory cytokines [27]. Microglia play a key role in this cascade; becoming activated after cytokine or glutamate exposure and, thereafter, serving to potentiate injurious processes [28, 29]. The loss or maturational delay of cellular targets results in hypomyelination or axonal damage, potentially causing conduction delay [30] and diminished neural function.

Areas of crossing WM tracts are proximal to affected periventricular sites and are vulnerable to WMI [31, 32]. Since these areas contain a variety of fibre populations with multiple cortical and subcortical targets, WMI has the potential to be extensive and, consequently, affect several functional domains. Grey matter structures such as the cortex, thalamus and basal ganglia, and the cerebellum are also affected by prematurity [12] and damage to these structures appears to occur in conjunction with WMI [33, 34].

Exploring premature white matter injury with neuroimaging

The high rate of neurocognitive impairment in the preterm population underscores the importance of early identification of individuals with WMI, both to prepare families for potential difficulties and for consideration of therapeutic intervention. Various neuroimaging modalities can detect WM abnormalities that predict adverse neurodevelopmental outcomes in preterm-born neonates. In the clinical setting, established methods include cranial ultrasound (c-US) and conventional (T_1 and T_2 -weighted) MRI. c-US is routinely used and is both accessible and cost-effective. Although it can successfully identify cystic WMI, it lacks sensitivity in recognising more diffuse, non-cystic pathology [35, 36].

Qualitative MRI findings include white matter abnormalities (WMA) such as focal regions of T_1 signal shortening or diffuse T_2 hyper-intensity, evidence of cystic change, lateral ventricular enlargement, corpus callosum thinning and a reduction in WM volume [35]. Increasing severity of WMA at term has been associated with WM microstructural disruption and poorer cognitive and motor performance at 2 years [37–42] and neonates with moderate-to-severe WMA are more likely to face serious cognitive and motor delays, including CP [43]. This approach, however, is limited by its subjective nature and lack of specificity in identifying infants with adverse outcomes.

Quantitative MRI studies of the WM have examined volumetric changes both globally across the whole brain as well as specific regional variation. During normal development, WM volume increases up to the fourth or fifth decade and is generally uniform between cortical lobes [44, 45]. This increase corresponds with continued axonal growth, glial proliferation and myelination, critical for the development of neurological function. In preterm-born individuals, the normal trajectory of cerebral WM growth is significantly diminished and specific differences are present in bilateral frontal, temporal, and parietal regions [46]. Volumetric differences have been identified in preterm infants through childhood and adolescence and have been related to neurodevelopmental aptitude [6]. Regionally, the corpus callosum has received much attention and reductions have been found in cross sectional area in preterm infants at term [47] and during adolescence [48, 49]. The splenium and other posterior regions appear to display the greatest differences and have been associated with tests of vocabulary [49] and verbal IQ [48]. The predominance of these posterior callosal regions is likely due to a number of factors including its late maturation [50] and proximity of susceptible periventricular oligodendrocytes [11]. Evidence suggests however, that gross WM damage in preterm infants is more widespread. Indeed, global WM volume reductions have been demonstrated in preterm children and adolescents compared to term-born controls, and have been associated with decreased intelligence and increased behavioural difficulties [51, 52]. In a large study of

preterm adolescents, WM loss was found in several regions including the brainstem, internal capsule, fronto-temporal regions and major fasciculi and was independently associated with cognitive and language impairments [53]. Still, volumetric WM changes are likely to be secondary to hypomyelination and axonopathy in preterm-associated WMI. Methods that examine WM microstructure should therefore provide a better approximation of the underlying neuropathology, and accurate quantification of microstructural damage may successfully predict neurological impairment.

d-MRI is particularly well placed as a neuroimaging biomarker to examine WM disruption in prematurity. The purpose of this paper is to review the use of d-MRI in prematurity. First, we define the key indices used in d-MRI and how these relate to normal and abnormal WM microstructure. Second, we outline the main analytical strategies currently employed in the preterm literature to quantify diffusion-based measures of WM microstructure and structural connectivity. Third, we offer a summary of findings of d-MRI related changes in preterms at term, during infancy, adolescence and adulthood and discuss how WM development is altered after premature birth. Finally, we explore the functional correlates of d-MRI based markers of WMI and their use in predicting later neurological impairment.

Diffusion MRI

Concepts and measures

Diffusion is the process which describes the random, thermally driven movement, or Brownian motion, of molecules over time. The diffusion profile of water molecules can vary across the brain due to highly complex biological structures. In the cerebro-spinal fluid (CSF), water molecules are allowed to move relatively freely. Diffusion is described here as being *isotropic*; that is, the average displacement of water molecules is equal in all directions. In the WM, water movement is restricted in certain directions by the presence of cellular architecture, causing diffusion to be *anisotropic*. The influence of cerebral tissue on water movement enables d-MRI to be highly sensitive to microstructural changes, including those changes associated with premature development and disease. Our attention is first given to the key diffusion indices used to assess cerebral microstructure and how they are generated.

In a sufficiently large and isotropic sample at a fixed temperature, diffusion can be described using the following equation [54]:

$$r^2 = 6Dt \quad (1)$$

where r , a Gaussian distributed random variable, describes displacement of the water molecules over time t , and D is the

diffusion coefficient of the medium. Since in vivo diffusion cannot be separated from other potential sources such as active transport and physiological pressure gradients, the diffusion coefficient is termed apparent diffusion coefficient (ADC) and is typically estimated through rearrangement of the following equation:

$$D = -\frac{1}{b} \ln\left(\frac{S}{S_0}\right) \quad (2)$$

where S and S_0 are the signal intensity values in the diffusion-weighted and reference (no diffusion encoding gradients) images, respectively, obtained from the phase gradient spin echo (PGSE) sequence. D is the diffusion coefficient (ADC) and can be calculated on a voxel by voxel basis. b is the diffusion-weighting variable and is calculated using Eq. 3 [55]:

$$b = \gamma^2 G^2 \delta^2 \left(\Delta - \frac{\delta}{3}\right) \quad (3)$$

where γ is the gyromagnetic ration for ^1H nuclei, and G , δ , and Δ are the strength, duration and time between diffusion gradients.

In the WM, ADC is strongly dependent on the direction of the encoding gradient [56]. The organisation of long neuronal axons in the white matter preferentially inhibits water diffusion such that it appears relatively unhindered when the encoding gradient is placed along the direction of a tract, but restricted when the gradient is placed orthogonal to the tract. The anisotropic signal reveals the ordered nature of the underlying structure of the WM (Fig. 1). Due to this rotational variance, capturing the behaviour of water molecules in the WM with a single gradient direction is inadequate. With a minimum of six gradient directions, the *diffusion tensor* offers us a more appropriate model to portray Gaussian diffusion, as shown in Eq. 4:

$$D = \begin{pmatrix} D_{xx} & D_{xy} & D_{xz} \\ D_{yx} & D_{yy} & D_{yz} \\ D_{zx} & D_{zy} & D_{zz} \end{pmatrix} \quad (4)$$

In this 3×3 symmetrical matrix, the diagonal elements of the tensor (D_{xx} , D_{yy} , D_{zz}) correspond to diffusivities along the orthogonal axes of the scanner. Isotropic diffusion can be modelled as a sphere, the size of which corresponds to the amount of displacement in a given time. In contrast, anisotropy is depicted with a skewed ellipsoid where the longest axis denotes the direction in which diffusion is greatest (Fig. 1). The values along each axis of the ellipsoid can be separated into directional and scalar components. The average diffusion distance along an axis is represented by a scalar magnitude known as the *eigenvalue*. The axes with the longest, middle

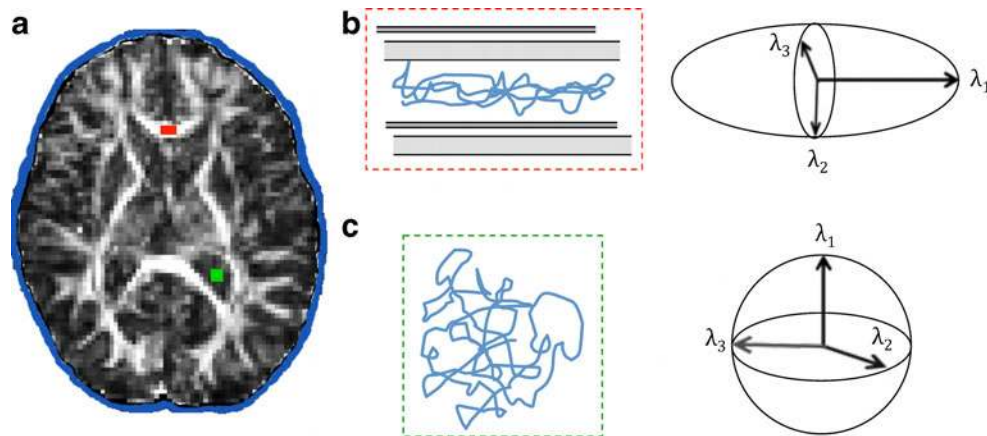


Fig. 1 Isotropic and anisotropic diffusion in the brain. Fractional anisotropy image of a preterm born child reveals the nature of water diffusion within different brain tissue compartments (**a**). In the white matter of the corpus callosum (*red*), diffusion occurs preferentially along the axonal fibres, resulting in anisotropic diffusion (**b**). In the ventricular cerebrospinal fluid (*CSF*; *green*), diffusion is unhindered and can be described as

isotropic (**c**). Diffusion tensor ellipsoids representing anisotropic and isotropic diffusion are shown in **b** and **c**, respectively. Each tensor is expressed by three eigenvectors with values λ_1 , λ_2 and λ_3 . In isotropic diffusion $\lambda_1 = \lambda_2 = \lambda_3$, whereas in anisotropic diffusion the long axis of the ellipsoid aligns with the underlying white matter, and λ_1 is greater than λ_2 and λ_3

and shortest magnitudes are denoted by λ_1 , λ_2 and λ_3 eigenvalues, respectively, and *eigenvectors* v_1 , v_2 and v_3 are their corresponding directional components. The average diffusivity across all three directions is known as the ‘total ADC’ or *mean diffusivity* (MD), as demonstrated in Eq. 5.

$$\text{MD} = \bar{\lambda} = \frac{\lambda_1 + \lambda_2 + \lambda_3}{3} \quad (5)$$

Diffusivity along the principal axis is known as principal or *axial diffusivity* (λ_{\parallel}), whilst the average of λ_2 and λ_3 is known as perpendicular or *radial diffusivity* (λ_{\perp}). *Fractional anisotropy* (FA) captures the degree to which the tensor ellipsoid is isotropic or anisotropic [57]. The calculation of FA is performed as shown in Eq. 6, and is normalized such that it takes values from zero (purely isotropic) to one (purely anisotropic).

$$\text{FA} = \sqrt{\frac{3}{2}} \frac{\sqrt{(\lambda_1 - \bar{\lambda})^2 + (\lambda_2 - \bar{\lambda})^2 + (\lambda_3 - \bar{\lambda})^2}}{\sqrt{(\lambda_1)^2 + (\lambda_2)^2 + (\lambda_3)^2}} \quad (6)$$

The tensor model represents one way of characterising diffusion among many; albeit still the most frequently used. It has certain limitations including its inability to account for non-Gaussian diffusion or detect anisotropy in regions of complex fibre organisation. In particular, in regions where multiple fibre populations converge or cross, other models of diffusion are better able to resolve the contribution of each to the anisotropic signal and account for uncertainty in the data. As an example, the ‘ball and stick’ model is a simplified partial volume representation of local diffusion and assumes that the anisotropic signal within a voxel exists along a single

dominant direction while the remainder represents isotropic, unhindered diffusion [58]. In voxels where multiple fibres are detected, the model extends naturally by including multiple ‘sticks’ in the model [59].

Neurobiological correlates of diffusion

The correlation between diffusion measures and the underlying neurobiology of WM is complex. Here, we offer examples from both WM development and disease, which relate microstructural components to specific diffusion measures.

ADC decreases exponentially during WM development, remains stable in adulthood and then gradually increases during senescence [60]. The developmental decrease in total water diffusivity is mainly due to loss of water, reduction in extracellular volume and increase in concentration of macromolecules such as myelin [61]. The increase in ADC in senescence is suggestive of demyelination, loss of axonal integrity, and a corresponding increase in extracellular volume [60].

Several intra- and extracellular factors appear responsible for the anisotropy observed in the WM. The axonal membrane is considered to be the primary and necessary determinant of anisotropy. Axons that are: normally non-myelinated; in a state prior to myelination; or are not forming myelin due to genetic mutations, all show anisotropy [62–64]. Myelin likely modulates the existing anisotropy: significant reductions in anisotropy are present in animal models of dysmyelination [62, 65] and elevated anisotropy corresponds to increased myelination in the developing postnatal WM [66, 67]. Pre-myelination processes such as the recruitment of oligodendrocyte precursors and the production of proteins required in myelination are also associated with elevated anisotropy [68]. Myelin associated changes in FA are principally due to alterations of λ_{\perp} rather than λ_{\parallel} . In contrast, axonal integrity is mostly associated

with λ_{\parallel} . Acute axonal damage is typically characterized by axonal degeneration with comparative myelin preservation and is related to reductions in λ_{\parallel} but not in λ_{\perp} [69], and decreased axonal area is associated with reductions in λ_{\parallel} [70].

In summary, these findings demonstrate that diffusion measures are a sensitive but unspecific marker of the neurobiological environment of WM.

Analysis methods

There are several analysis methods used to compare d-MRI measures between different groups or in the same group over time. A key consideration in all these methods is to ensure that a ‘like for like’ comparison is made (i.e., that the examined areas are anatomically correspondent). d-MRI studies may investigate differences in one or more well-defined regions or fibre tracts, or across the entire WM. Below, we discuss the main approaches which have been applied in d-MRI studies of preterm-born individuals and highlight the key advantages and limitations of each.

Region of interest (ROI) approaches compare d-MRI measures in specific anatomical areas, defined a priori. Regions are usually delineated manually by an expert and can serve as a gold standard for comparison against other methods. ROI approaches are widely available, applicable for use in individual patients and avoid a multiple comparison problem when studying a limited number of regions. In spite of these benefits, manual delineation can be very time consuming in large samples, and can suffer from low repeatability and high variability [71, 72], the latter being a salient concern in the preterm population [73]. Automated segmentation methods overcome some of these limitations. ROIs are delineated by mapping the anatomical information from an *atlas*, or previously manually segmented brain, onto a *target* or subject brain. Underpinning this mapping procedure are *registration* algorithms, which attempt to align the anatomy of the atlas with the target; and the propagation of label information from the atlas to the target image. By combining the information of multiple atlases to segment each subject, ROIs created by automated approaches can show a high degree of similarity to manual gold standards [74].

Voxel-based morphometry (VBM) can be applied to diffusion data and permits a global survey of WM, where diffusion parameters in homologous voxels are compared across subject images [75]. Applying registration methods, images are first spatially normalised to a common stereotactic space. Normalised images are then partitioned according to tissue class, and the cerebral white matter is extracted [76]. This area is subsequently thresholded to ensure that grey matter or CSF do not cause partial voluming errors and is corrected for registration errors by *smoothing*: a process which averages the values from a single voxel with its nearest neighbours. Statistical analyses are performed at a voxel-wise level to localise and

make inferences about group differences or detect associations with particular effects under study. Given the number of white matter voxels and therefore the large number of tests, multiple comparison correction is needed to find areas with significant differences and reduce Type I error. VBM methods are effective in exploring local WM differences, which are not hypothesised a priori and like other global methods, it can be automated and is time-efficient. However, this approach is susceptible to artefacts and errors of normalisation and lacks a principled way of choosing the degree of smoothing.

Tract-based spatial statistics (TBSS) shares some key features of VBM: it studies WM across the whole brain and detects differences at a voxel-wise level [77]. In TBSS, the FA images of group individuals are aligned to a common space and averaged. A WM skeleton is created which contains voxels at the centre of fibre tracts, common to all group members. This common skeleton is thresholded such that regions with low mean FA and high inter-subject variability are excluded. An FA skeleton for each subject is produced by performing a perpendicular search for the maximum FA value and local tract centre, and projecting it onto the common skeleton (Fig. 2). Voxel-wise statistics are then performed across subjects on the skeleton space FA data. TBSS shares many of the advantages that VBM offers, and also demonstrates low variability and high confidence that FA values are taken from relevant voxels. Examining a sparse number of voxels in a tract skeleton as compared to the entire white matter allows TBSS to have increased statistical power. However, this comes at the cost of restricting the examination to the major WM pathways.

Diffusion tractography estimates and visualises the trajectory of WM fibres. By inferring the fibre orientation from directional information at individual voxels, a ‘tract’ can be sequentially pieced together. Tractography algorithms start tracing from a set of voxels known as a *seed* region, and arrest upon contact with a *target* set of voxels or by meeting a stopping criterion such as contact with GM or CSF. There are two principal methods by which tractography can be performed. *Deterministic* algorithms propagate streamlines from seed regions along the principal orientation (eigenvector v_1) in a voxel by voxel manner [78] (Fig. 3a). Streamlines terminate upon reaching a point where anisotropy is too low or when the angle created by the principal orientations of adjacent voxels in the path of the streamline voxels exceeds a critical threshold. Although this approach is able to reconstruct tracts with high accuracy and fidelity [79], it is limited in regions where there are crossing fibre populations or where the orientation of the fibre population is uncertain. *Probabilistic* approaches can deal with this limitation by calculating a distribution of probable fibre orientations for each voxel after estimating the uncertainty between the diffusion model and the signal [59] (Fig. 3b). Tractography enables a comparison of corresponding fibre populations between individuals, even if

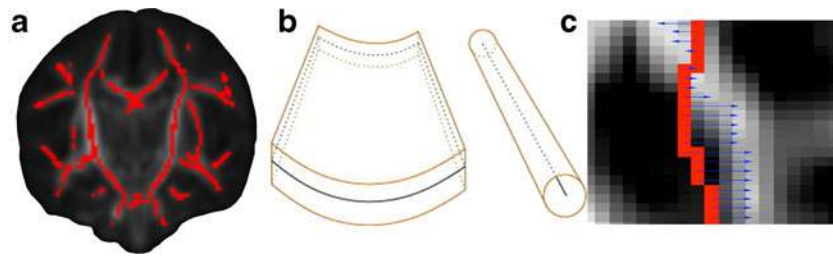


Fig. 2 Generating the FA skeleton in TBSS. White matter tracts are thinned to form a FA skeleton (**a**) comprising a set of sheets or tubes that represent the topology of the white matter and contain voxels from the

centre of the tracts (**b**). Individual FA values are then projected from transformed maps onto the group skeleton, in order to reduce the effect of misregistration (**c**). Modified from Fig. s2 in [77]

the precise location of a tract varies. To calculate diffusion measures in all or part a tract, the space occupied by the fibre bundle is parameterised and an average is taken across voxels. The estimated volume of a tract and the characteristics of its spatial trajectory are also frequently reported. Some approaches may be combined together. For instance, VBM or TBSS may first be employed to survey the white matter for areas of significant change. These areas in turn may be further

examined using ROI methods, or one may wish to perform tractography to accurately identify the affected tracts which pass through this area.

Diffusion MRI and preterm birth

Effect of prematurity at birth or term-equivalent age

d-MRI studies assessing preterm infants shortly after birth or at term-equivalent age (TEA) have detected several WM structures that appear to be affected by prematurity (Table 1). These WM areas undergo extensive maturation and myelination approaching the time of birth [80, 81] and are potentially vulnerable to pathology associated with prematurity. A whole-brain study of late preterm neonates shortly after birth, found that FA in the thalami, posterior and anterior limbs of the internal capsule (ALIC, PLIC), centrum semiovale (CSO) and optic radiations (OR) was positively associated with gestational age (GA) [82]. At TEA, reduced FA was found in the CSO, frontal white matter, sagittal striatum and corpus callosum (CC) as compared to term-born controls [83–85] and extended to the PLIC, external capsule (EC) and posterior aspects of the CC with greater prematurity [83]. Region- and tract-specific approaches were consistent with these findings. Increased ADC and reduced anisotropy were associated with the length of prematurity in the PLIC, CC and thalamo-cortical pathways [66, 85–87] (Fig. 4). In the above studies, preterm-born subjects with focal abnormalities on structural MRI or had positive findings using cUS were excluded. This suggests that microstructural WM changes are associated with the degree of prematurity, independent of the presence of WM lesions or macrostructural pathology.

WMI has also been found to impact upon the *rate* of WM development. Two studies found that the normal tempo of WM development in this population is also affected. A small sample study found that the normal maturational increase in anisotropy was absent in the frontal WM of infants with mild conventional imaging abnormalities and in several regions in infants with moderate abnormalities [88]. A longitudinal study examining the cortico-spinal tract (CST), revealed that

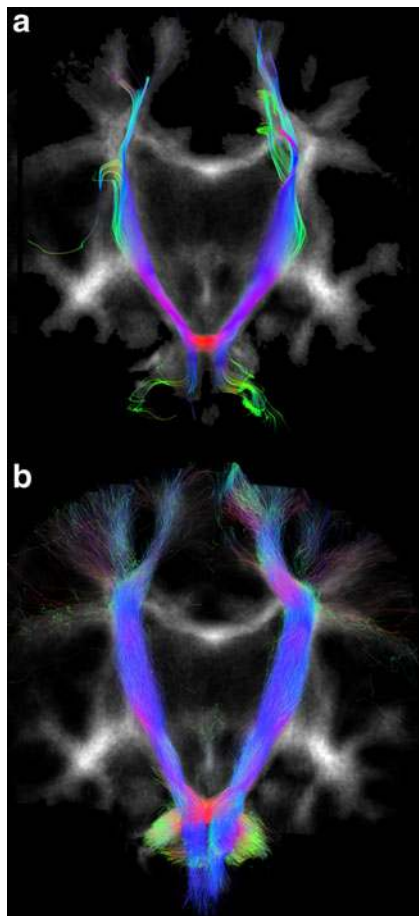


Fig. 3 Deterministic and probabilistic tractography. The cortico-spinal tract is delineated in a preterm infant at term-equivalent age with deterministic (**a**) and probabilistic (**b**) tractography. Diffusion is modelled voxelwise with the diffusion tensor in **a**, and with constrained spherical deconvolution, to account for multiple fibre directions, in **b**

Table 1 d-MRI studies of preterms at birth of term equivalent age

Author	Demographics	Additional PT criteria	Scanning Details	d-MRI analysis	Neurological outcome(s)	Key findings
Groppo et al. 2012 [105]	PT: <i>n</i> =53, median GA at birth=30.1 weeks (25.6–34.9), BW=1,260 g (745–1,690), scanning age=40.9 weeks (39.3–46), <i>n</i> =22 had early scan at 32.7 weeks (29.7–36)	Inclusion criteria: <36 weeks GA and successful completion of visual assessment	3 T, 32 days, <i>b</i> =750, slice thickness=2 mm	Tractography (probabilistic)	Visual Function (at 2 years), SDQ (at 5 years)	↑ FA in OR at TEA associated with ↑ visual function, GA at birth and PMA at scan. In a sub-group of neonates with scanning at birth, visual function was predicted by FA at term and rate of increase in FA between birth and term but not FA at birth.
Rogers et al. 2012 [134]	PT: <i>n</i> =111, GA at birth=27.6 weeks, BW=980 g, scanning age=40.1 weeks	Inclusion criteria: <30 weeks GA or 1,250 g. Exclusion criteria: congenital abnormality, severe CP, death, inaccessible to follow-up, 17 % PT had moderate-severe MRI abnormalities	1.5 T, 6 days, <i>b</i> =700, slice thickness=4–6 mm	ROI	ITSEA (at 2 years), SDQ (at 5 years)	↑ ADC in the right OFC associated with ↑ social-emotional difficulties at 5 years; - ↓ hippocampal volume associated with hyperactivity, peer problems and SDQ total score in PT females whilst ↓ frontal region in PT males associated with ↓ prosocial score; - Only PT female - hippocampal finding was significant in multivariate analysis and was associated with problems in similar domains at 2 years
Lepomaki et al. 2012 [73]	PT: <i>n</i> =27, GA at birth=30 weeks, BW=1,481 g, scanning age=39.9 weeks; SGA: <i>n</i> =9, GA at birth=31.6 weeks, BW=1,294 g, scanning age=40 weeks	Inclusion criteria: <32 weeks GA or 1,500 g. Exclusion criteria: death, lived outside hospital district, chromosomal abnormalities, brain infection, did not speak Finnish or Swedish, WM cysts, HPI, IVH grade III/IV, ventriculitis, any MRI abnormalities (WMA)	1.5 T, 15 days, <i>b</i> =600/1,200, slice thickness=5 mm	TBSS	-	↓ FA in bilateral ATR, CST, Fm9j, Fmin, IFOF, ILF, SLF, UF in SGA group vs. AGA. - No association between FA or ADC and GA at birth in either group
van Pul et al. 2012 [42]	PT: <i>n</i> =89, mean GA=28.5 weeks, BW=1,121, PM scanning age=41.7 weeks (39.6–44.7) (<i>n</i> =85 with PLIC data, <i>n</i> =72 with CC data)	Inclusion criteria: ≤31 weeks GA. Exclusion criteria: chromosomal abnormalities, brain infection. 11 % PT had no WMA, 74 % had mild WMA and 14 % had moderate-severe WMA	3 T, 32 days, <i>b</i> =800, slice thickness=2 mm	Tractography (deterministic)	-	↑ WMA score associated with ↓ FA, bundle length, bundle volume and ↑ ADC, λ_{\perp} , λ_{\parallel} in the CC; ↑ ADC, λ_{\perp} , λ_{\parallel} in left PLIC and ↑ ADC, λ_{\perp} in right PLIC; - ↑ GA at birth associated with ↑ CC bundle volume and length; ↓ FA and ↑ ADC, λ_{\perp} , λ_{\parallel} in left PLIC; ↑ bundle volume and length in right PLIC; .Comparing no WMA vs. mild WMA: ↓ FA in left sensory STR; ↑ ADC in left ATR, left sensory STR, bilateral motor STR; ↑ λ_{\perp} in left ATR, left sensory STR, bilateral motor STR, right CST.
Liu et al. 2012 [41]	PT: <i>n</i> =70	Exclusion criteria: congenital malformation, infection, 59 % PT with no WMA, 39 % with mild WMA, 3 % with moderate WMA.	1.5 T, 32 days, <i>b</i> =600, slice thickness=2.3 mm	Tractography (probabilistic)	BSD-II	↑ WMA score related to ↓ FA values in CC genu, anterior midbody and whole. - ↓ GA associated with ↓ CC tract volume. - ↑ BSD-PDI associated with ↓ ADC and λ_{\perp} in the CC splenium
Thompson et al. 2012 [40]	PT: <i>n</i> =106, GA at birth=27.6 weeks, BW=996 g, PM scanning age=40 weeks (38–42)	Inclusion criteria: <30 weeks GA and/or 1,250 g. Exclusion criteria: congenital abnormalities, 5 % of PT had IVH grade III/IV, 68 % had at least mild MRI abnormalities (WMA), 15 % with moderate to severe MRI abnormalities, 8 % with CP at 2 years	1.5 T, 6 days, <i>b</i> =700, slice thickness=4–6 mm	Tractography (probabilistic)	BSD-II	↑ WMA score related to ↓ FA values in CC genu, anterior midbody and whole. - ↓ GA associated with ↓ CC tract volume. - ↑ BSD-PDI associated with ↓ ADC and λ_{\perp} in the CC splenium
Ball et al. 2013 [156]	PT: <i>n</i> =47, median GA at birth=28.4 weeks (23.6–34.9), median PM at scan=41.4 weeks (38.3–44.1)	Inclusion criteria: <36 weeks GA. Exclusion criteria: cystic PVL, HPI	3 T, 32 days, <i>b</i> =750, slice thickness=2 mm	Tractography (whole-brain probabilistic)	-	↓ Anisotropy in connections between the thalamus and the frontal cortices, supplementary motor areas, occipital lobe and temporal gyri in PT group compared to controls.

Table 1 (continued)

Author	Demographics	Additional PT criteria	Scanning Details	d-MRI analysis	Neurological outcome(s)	Key findings
Ball et al. 2012 [87]	Controls: $n=18$, median GA at birth=39.3 weeks (36–41.9), BW=1,110 g (630–2,370), median PM at scan=39 weeks (41.9–44.6) PT: $n=71$, median GA at birth=28.7 weeks (23.6–35.3), BW=1,110 g (630–2,870), median PM at scan=41.7 weeks (38.1–44.6 weeks)	Inclusion criteria: <36 weeks GA. Exclusion criteria: cystic PVL, HPI, 11.3 % PT with punctate WM pathology	3 T, 15 days, $b=750$, slice thickness=2 mm	TBSS	–	↓ GA associated with ↓ volume in thalamus, hippocampus, orbitofrontal lobe, posterior cingulate cortex, and centrum semiovale. - ↓ volume in thalamus associated with ↑ thalamic ADC and with ↓ FA, ↑ λ_x in PLIC and CC. - ↓ volume in cortex associated with ↓ FA, ↑ λ_x in posterior CC
Bassi et al. 2011	PT with punctate lesions: $n=23$, median GA=30 weeks (25.4–35.3), BW=1,250 g (860–2,500), PM scanning age 1=30 weeks (27–34.4 weeks), PM scanning age 2=41 weeks (39–43.3) PT without punctate lesions: $n=23$, median GA=30 weeks (25.1–35.1), BW=1,320 g (690–2,170), PM scanning age 1=30 weeks (26.7–35.7), PM scanning age 2=41.4 weeks (39–43.3)	Inclusion criteria: <36 weeks GA. Exclusion criteria: cystic PVL, HPI	3 T, 15 days, $b=750$, slice thickness=2 mm	TBSS, Tractography (probabilistic)	–	↑ GA associated with ↑ FA in CC, PLIC, ILF, OR, left frontal WM. - ↑ FA in CST associated with ↓ number of lesions in PT-lesion group at TEA. - ↓ FA in PT-lesion group compared to PT controls in PLIC, cerebral peduncles, decussation of the SCP, SCP, and pontine crossing tract
Hasegawa et al. 2011 [85]	PT: Group A – $n=10$, GA at birth=24.7 weeks (23–25.9), BW=718 g (554–932), corrected scanning age=40.4 weeks (38–43.7); Group B – $n=23$, GA at birth=28.1 weeks (26.1–29.7), BW=973 g (556–1,405), corrected scanning age=40.1 weeks (37.4–43.7); Group C – $n=25$, GA at birth=32.1 weeks (30.1–33.7), BW=1,425 g (706–2,012), corrected scanning age=39.2 weeks (37.9–43.7)	Inclusion criteria: 34 weeks GA at birth, no evidence of PVL and grade III–IV IVH on cUS or MRI, scanning at TEA (37–43 weeks corrected GA).	1.5 T, $b=1,000$, slice thickness=2.5 or 3 mm	Tractography (deterministic), ROI	–	↓ FA in tract(s) passing through splenium in A and B vs. C. - ↓ FA in isthmus ROI in groups A and B vs. C and in splenium ROI for group A vs. B and C. - Cross-sectional area of isthmus ROI was ↓ in A vs. C and for splenium ROI was ↓ A vs. B and C. - ↑ GA associated with ↑ FA in isthmus ROI, splenium tracts and ROI
Bonifacio et al. 2010 [39]	PT: $n=176$ from 2 sites ($n=97$ and $n=79$), GA at birth=28.4 and 27.3 weeks, BW=950 g (750–1,220) and 995 g (815–1,285), scanning age 1=32 weeks (30.7–33.1) and 32 weeks (30.3–33.6), scanning age 2=36 weeks (35.1–37.3) and 40 weeks (38.4–42.6)	Inclusion criteria: 24–33 weeks. Exclusion criteria: congenital malformation, antenatal infection, large parenchymal haemorrhagic infarction (>2 cm) on cUS, 31 % of PT from site 1 and 35 % from site 2 had moderate–severe MRI abnormalities	1.5 T, 12 days, $b=600$ or 700, slice thickness=3 mm	ROI	–	Birth <26 weeks associated with ↓ WM FA but not after accounting co-morbidity. - Moderate–severe brain injury associated with ↓ WM FA
Adams et al. 2010 [38]	PT: $n=55$, median GA at birth=27.6 weeks (24–32), BW=9g, median scanning age 1=32 weeks, median scanning age 2=40.3 weeks	Exclusion criteria: congenital malformation, antenatal infection, large HPI (>2 cm) on cUS, 38 % of PT have moderate–severe MRI findings on scan 1 or 2	1.5 T, 12 days, $b=600$ or 700, slice thickness=3 mm	Tractography (deterministic)	–	PT with abnormal MRI had slower FA increase rate in CST as compared to normal PT. ↑ ADC in PT with abnormal MRI. Postnatal infection related with slower FA increase rate after adjusting for PT group.
Skjold et al. 2010 [160]	PT: $n=54$, GA at birth=25.6 weeks (23.1–26.9), BW=809 g (494–1,161), scanning age=TEA (39–41) Normals: $n=16$	Inclusion criteria: <27 weeks GA. Exclusion criteria: chromosomal abnormalities, metabolic or malignant disorders, congenital malformations or infection, 4 % PT with IVH III, 86 % with no-mild WMA, 14 % with moderate–severe congenital malformations or infection, syndromic	1.5 T, 15 days, $b=700$, slice thickness=22 mm	ROI	–	PT with normal appearing WM had ↓ FA and ↑ higher ADC in the CC compared to controls. - In the CSO, PT with WM abnormalities or DEHSI had ↓ FA and ↑ ADC compared with controls
Glass et al. 2010 [104]	PT: $n=9$ with 15 scans, GA at birth=28.9 weeks, BW=1,115 g (875–1,840), scanning	Inclusion criteria: <34 weeks GA. Exclusion criteria: congenital malformations or infection, syndromic	Tractography (deterministic)	–	–	↑ Peak response amplitude for spatial frequency associated with ↑ FA, ↓ ADC and λ_x

Table 1 (continued)

Author	Demographics	Additional PT criteria	Scanning Details	d-MRI analysis	Neurological outcome(s)	Key findings
Liu et al. 2010 [41]	age 1=33.1 weeks (31–34.7), scanning age 2=37.6 weeks (32.9–40.1), neurodevelopmental assessment at 30 months (14–37). PT: n=27, median GA at birth=30.7 weeks (26–34.4), median corrected scanning age=36.9 weeks (35.4–42.1)	diagnosis, ROP>stage 2. All PT had normal cognitive subscales Inclusion criteria: normal weight and head circumference for GA, 5-min Apgar<6, lack of congenital abnormality/infection, normal conventional MRI findings, normal physical and neurological findings at term and 24 m	1.5 T, 6 days, b=700, slice thickness=3 mm 1.5 T, 32 days, b=600, slice thickness=2.3 mm	Tractography (probabilistic)	BSD-III, Visual-evoked potential	Trend for leftward asymmetry for CST in terms of ↑ volume and FA, ↓ ADC and λ_{\perp} - significant L>R asymmetry for f motor-STR volume, parieto-temporal SLF volume and FA
Baill et al. 2010 [142]	PT: n=93, median GA at birth=28.7 (23.6–35.3 weeks), median BW=1,100 g (630–3,710), median scanning age=41.6 weeks (38.1–46.9 weeks)	Inclusion criteria: <36 weeks GA. Exclusion criteria: cystic PVL or HPI on TEA MRI, 20.4 % with CLD	3 T, 15 days, b=750, slice thickness=2 mm	TBSS	–	PT with CLD had ↓ FA in bilateral ILF, CSO, CC and left EC, ↑ λ_{\perp} in bilateral ILF, IC, CSO, CC genu and splenium and left EC. - ↑ Length of respiratory support associated with ↑ FA, λ_{\parallel} and λ_{\perp} in widespread regions across the skeleton. - ↑ GA associated with ↑ FA, ↓ λ_{\parallel} and λ_{\perp} in widespread regions across the skeleton
Aeby et al. 2009 [82]	PT: n=22, GA at birth=36.3 weeks, scanning age between 31 and 41 weeks, all healthy Controls: n=6, GA at birth=39.4 weeks	Inclusion criteria: normal weight and head circumference for GA, 5-min Apgar<6, lack of congenital abnormality/infection, normal conventional MRI findings, normal physical and neurological findings at term and 24 m, normal psychomotor development findings at 24 m	1.5 T, 32 days, b=600, slice thickness=2.3 mm	VBM, Tractography (probabilistic)	–	↑ GA linearly associated with FA in clusters involving: bilateral thalami, ALIC, PLIC, OR, CSO. - Principal fibre tracts running through these clusters: CST, ATR, STR, PTR, CR
Cheong et al. 2009 [37]	PT: n=111, GA at birth=27.4 weeks, BW=992 g, scanning age=40.2 weeks	Inclusion criteria: <30 weeks GA or <1,250 g, 5.4 % of PT had IVH grade III/IV and 4.5 % had cystic PVL, 35 % had normal conventional MRI, 53 % with focal WMSA and 12 % with extensive WMSA.	1.5 T, 6 days, b=700, slice thickness=4–6 mm	ROI	–	PT with extensive T1/T2 signal abnormalities had ↑ ADC in bilateral sensorimotor and right superior occipital ROI and ↓ λ_{\parallel} in bilateral sensorimotor and right IC vs. normal PT. - Compared with normal or focal WMSA PT, normal PT had ↓ FA in bilateral IC, right frontal and superior-occipital and ↑ λ_{\perp} in bilateral sensorimotor and right inferior frontal, IC, superior occipital.
Anjari et al. 2009 [141]	PT: n=53, median GA at birth=28.3 weeks (24.3–34.6), median BW=3,400 g (2,000–5,500), median scanning age=42 weeks (38.1–44.3)	Exclusion criteria: cystic PVL or HPI on TEA MRI, 18.9 % PT with ALD, 28.3 % with CLD, 28.3 % with evidence of infection	3 T, 15 days, b=750, slice thickness=2 mm	TBSS	–	↑ GA associated with ↑ FA in CC splenium and posterior-body, left PLIC, frontal WM, inferior longitudinal WM. - ↓ FA in CC genu in ALD vs. normal PT. - ↓ FA in left ILF in CLD vs. normal PT.
Berman et al. 2008 [103]	PT: n=36, GA at birth=28.4 weeks (20.3–33.1), scanning age=34.5 weeks (29–41)	58 % of PT had no periventricular WM abnormality on conventional MRI, 25 % had minimal, 11 % had mild, 6 % had moderate.	1.5 T, 6 days, b=600, slice thickness=3 mm.	Tractography (deterministic)	Visual Function: gaze fixation	↑ Visual fixation performance correlated with ↑ FA in OR
Bassi et al. 2008 [102]	PT: n=37, median GA at birth=28.6 weeks (24.1–32.4), BW=1,059 g (655–1,528), scanning age=42 (39.9–43)	Inclusion criteria: ≤34 weeks GA with no congenital or chromosomal abnormalities or metaboloid disorders. Exclusion criteria: focal lesions (MCA infarction, HPI), 21.6 % ROP positive, 27 % with MR lesions	3 T, 15 days, b=750, slice thickness=2 mm	Tractography (probabilistic), TBSS	Visual Function	↑ Visual assessment score correlated with ↑ FA in OR - TBSS confirmed correlation only with FA in OR not other WM areas
Rose et al. 2009 [124]	VPT: n=12, GA at birth=26.9 weeks (25–29), BW=1,022 g, scanning age=41.1 weeks; PT:	Exclusion criteria: cortical or WM injury, haemorrhage, brain malformation, chromosomal	1.5 T, b=1,100, slice thickness=2.5 mm	TBSS, ROI	–	↓ FA in the sagittal striatum, frontal WM, CC, EC and CSO in VPT vs. PT. - VPT vs. term showed ↓ FA in same regions as previous and also in CC

Table 1 (continued)

Author	Demographics	Additional PT criteria	Scanning Details	d-MRI analysis	Neurological outcome(s)	Key findings
Giminez et al. 2008	$n=11$, GA at birth=30.9 weeks (29–32), BW=1,530 g, scanning age=41.1 weeks Controls: $n=10$, GA at birth=39.5 weeks (37–42), BW=3,353 g, scanning age=39.8 weeks PT: $n=27$, GA at birth=31 weeks (28–34), BW=1,554 g (800–2,160), scanning age=41 weeks (38–46) Controls: $n=10$, GA at birth=39 weeks (37–42), BW=3,259 g (2,000–4,336), scanning age=40 weeks (38–42)	abnormality, congenital infection on conventional MRI.	3 T, 6 days, $b=1,000$, VBM slice thickness=3.4 mm	–	–	splenium and CR and \uparrow FA in the CST, which is also seen in PT vs. term. \uparrow FA in bilateral sagittal striatum in PT vs. controls.
Drobyshevsky et al. 2007	PT: $n=21$, GA at birth=28.7 weeks (24.1–30.9), BW=1,244 g (640–1,716), scanning age 1=30.4 weeks (25.9–32.9), scanning age 2=35.7 weeks (34.1–37.1)	Inclusion criteria: <32 weeks GA, 19 % of PT had severe brain injury (IVH grade III/IV or cystic PVL), 29 % had mild brain injury (IVH grade I/II) and 52 % were without abnormalities on cUS and MRI	6 days, $b=1,000$, ROI slice thickness=5 mm	ROI	BSD-II (at 2 years)	\uparrow ADC of scan 2 in central and occipital WM, CR; \downarrow FA in OR in severe PT vs. normal PT. - \downarrow ADC of scan 2 in central and occipital WM in mild PT vs. controls. - \uparrow FA in PLIC on scan 1 in sub-group ($n=12$) associated with \uparrow PDI score. - \downarrow PDI associated with \uparrow Δ FA/week in IC, occipital WM associated with \uparrow ADC associated with \uparrow DQ. - \uparrow ADC in PT with postnatal sepsis
Krishnan et al. 2007	PT: $n=38$, median GA at birth=31 weeks (25–34), BW=1,330 g (692–2,266), median scanning age=40 weeks (38–44)	Inclusion criteria: ≤ 34 weeks GA. Exclusion criteria: cystic PVL, HPI, post-haemorrhagic hydrocephalus. All PT normal functioning, 21.1 % with postnatal sepsis.	1.5 T, $b=1,000$, slice thickness=5 mm	ROI	GMDS (AT 2 years)	\downarrow ADC associated with \uparrow FA in bilateral PLIC
Dudnik et al. 2007 [86]	PT: $n=28$, GA at birth=28.7 weeks (26–32), BW=1,148 g	Inclusion criteria: 25–32 weeks GA, no evidence of WMI on conventional MRI and scanned within 4 days of birth. Exclusion criteria: IVH, VM, congenital infection or malformation.	1.5 T, 25 days, $b=1,000$, slice thickness=3 mm	Tractography (deterministic)	Denver score, BSD-II (at 2 years)	\uparrow GA associated with \uparrow FA in bilateral PLIC
Aijani et al. 2007 [83]	PT: $n=26$, median GA at birth=28.9 weeks (25.7–32.6), median BW=1,084 g (654–1,848), scanning age=41.3 weeks (38.1–45.3); EPT: $n=11$ <28 weeks, median GA at birth=26.7 weeks (25.7–28.0), median BW=920 g (714–1,200), scanned at 41 weeks (38.1–44) Controls: $n=6$, median GA at birth=39.7 weeks (39–40.6), BW=3,300 g (3,106–4,000), scanning age=41.7 weeks (41–46)	Exclusion criteria: focal lesions including cystic PVL and HPI on conventional MRI	3 T, 15 days, $b=750$, slice thickness=2 mm	TBSS, ROI	–	\downarrow FA in CSO, frontal WM, CC genu in PT vs. controls. - \downarrow FA in same regions but also in posterior PLIC, EC, isthmus, CC body in EPT vs. controls
Counsell et al. 2006 [161]	PT: $n=38$, median GA at birth=30 weeks (25.1–34), median BW=1,348 g (610–2,226), scanning age=40.4 weeks (38.9–43.9) Controls: $n=8$, median GA at birth=39.3 weeks, median BW=3,520 g (3,216–4,700), median scanning age=41 (38.6–41.3)	Exclusion criteria: overt WMI lesions such as PVL and HPI. 76 % of PT had DEHSI, 24 % had normal appearing WM on conventional MRI. 11 % had IVH on cUS	1.5 T, 6 days, $b=710$, ROI slice thickness=5 mm	ROI	–	\uparrow λ_s in posterior PLIC, CC splenium and \uparrow λ_s , λ_{q1} in CSO, frontal WM, periventricular WM, occipital WM in PT vs. non-DEHSI PT and controls
Partridge et al. 2004 [64]	PT: $n=14$, median GA at birth=29 weeks (28–39) of which $n=8$ had serial scan, scanning age 2=37.5 weeks (35–43)	Inclusion criteria: 24–36 weeks GA with no evidence of WMI on conventional MRI. Exclusion criteria: IVH>grade I, congenital infection or malformation.	1.5 T, 6 days, $b=600$, slice thickness=3 mm	ROI	–	\uparrow age associated with \uparrow FA, \downarrow ADC, λ_s , λ_{q1} in several WM regions. - Serial data showed that CSO had greatest rate of change
Arzoumanian et al. 2003 [162]	PT: $n=63$, all ≤ 33 weeks GA at birth, all <1,800 g BW, scanning age=37 weeks (34.2–42.2 weeks)	Inclusion criteria: ≤ 33 weeks GA, BW <1,800 g with no congenital malformation. Exclusion criteria: macrostructural abnormalities on	1.5 T, 6 days, $b=1,000$, slice thickness=4 mm	ROI	Amiel-Tison neurological examination,	PT who later developed abnormal neurological outcomes including CP had \downarrow FA in bilateral PLIC

Table 1 (continued)

Author	Demographics	Additional PT criteria	Scanning Details	d-MRI analysis	Neurological outcome(s)	Key findings
Miller et al. 2002 [88]	Normal PT: $n=11$, GA at birth=29.2 weeks (25–31.8), BW=1,210 g (700–1615), scanning age 1=31.5 weeks (27.5–38), scanning age 2=37.4 weeks (35.1–43); PT with minimal WMI: $n=7$, GA at birth=31 weeks (26.6–33.8), BW=1,580 g (1,040–2,145), scanning age 1=34.4 weeks (30.9–35), scanning age 2=37.3 weeks (35.7–42.4); PT with moderate WMI: $n=5$, GA at birth=30 weeks (26.6–31.8), BW=1,020 g (1,040–2,145), scanning age 1=31.4 weeks (31–36), scanning age 2=36 weeks (33.2–42.1)	conventional MRI: 68 % of PT had no abnormality, of which 26 % had abnormal neurologic outcome (incl CP). 32 % of PT had minimal subependymal haemorrhage or mineralisation of which 10 % had abnormal neurologic outcome Inclusion criteria: <36 weeks GA. Exclusion criteria: congenital malformation or infection, HPI on cUS, T1/T2 foci of haemorrhage	1.5 T, 6 days, $b=600$, ROI slice thickness=3 mm	ROI	gross motor skill assessment at 2 years	Maturation increase in anisotropy was present in all WM regions in normal PT; only in frontal region of PT with minimal WMI; and absent in widespread regions in PT with moderate WMI
Huppi et al. 2001 [163]	PT: $n=10$, GA at birth=29 weeks, BW=1,294 g, PT with abnormal MRI: $n=10$, GA at birth=29.2 weeks, BW=1,318 g. Both groups scanned at term	Inclusion criteria: <32 weeks GA	1.5 T, 7 days, $b=700$, ROI slice thickness=7.3 mm	ROI	–	PT with abnormal MRI had ↓ anisotropy in PLIC and central WM
Huppi et al. 1998 [66]	PT: $n=17$, GA at birth=30.9 weeks (25–35), of which VPT: $n=10$, GA at birth=28.8 weeks (25–31), scanning age=39.9 weeks (38–42) Controls: $n=7$, GA at birth=39.4 weeks (38–40)	Inclusion criteria: stable respiratory status, normal cUS, normal neurology examination, appropriate weight for GA, no congenital malformations	1.5 T, 7 days, $b=700$, ROI slice thickness=7.3 mm	ROI	–	PT at term showed ↑ ADC in central WM and ↓ anisotropy in PLIC and central WM
van Kooij et al. 2012 [113]	PT: $n=63$, GA at birth=28.7 weeks (25.1–30.9), BW=1,146 g (650–1,910), scan age [PMA]=41.6 weeks (39.6–44.7)	Inclusion criteria: PT <31 weeks GA. Exclusion criteria: congenital malformations or brain infection. 7.9 % with IVH grade III/IV on cUS. 85.7 % PT with normal–mild WMA on conventional MRI, 14.3 % with moderate abnormalities.	3 T, 32 days, $b=800$, TBSS, ROI slice thickness=2 mm	ROI	BSD-III (at 2 years)	↑ Cognitive subscale score associated with ↑ FA, $\lambda_{ }$ in CC body and splenium. - ↑ Fine motor associated with ↑ FA in CC and bilateral fornix, CR, EC, CST, SLF, ILF, IFOF and right CG and UF; ↑ Fine motor associated with ↓ λ_{\perp} in right PLIC, left CST; and $\lambda_{ }$ in left PLIC. - ↑ Gross motor associated with ↑ FA in the left PLIC and thalamus; with ↓ λ_{\perp} in the fornix, CC, PLIC and posterior CG; with ↑ $\lambda_{ }$ in the left PLIC. - ↑ Total motor associated with ↑ FA in the CC and bilateral fornix, CR, EC, CST, SLF, ILF, IFOF, CF, UF; and ↓ λ_{\perp} in the CC, fornix, left EC, ILF, IFOF, UF and bilateral CST
de Bruine et al. 2011 [164]	PT: $n=84$, GA at birth=29 weeks (25.6–31.9), scanning age [PMA]=45 weeks (40.0–62.1)	Inclusion criteria: PT ≤32 weeks GA. Exclusion criteria: congenital brain abnormalities. 21 % PT were classified with normal–mild WMA on conventional MRI, 61 % with moderate and 18 % with severely abnormal WM	3 T, 32 days, $b=1,000$, slice thickness=2 mm	Tractography (deterministic)	–	No association between FA or ADC in PLIC or CC, with GA at birth or degree of WMI
Reiman et al. 2009 [107]	PT <32 weeks GA, BW ≤1,500 g, parents spoke Finnish or Swedish and lived in the	Inclusion criteria: PT <32 weeks GA, BW ≤1,500 g, parents spoke Finnish or Swedish and lived in the	ROI	ROI	Brainstem auditory-	Shorter BAEP wave I, III, and V latencies and I–III and I–V intervals and higher wave V amplitude

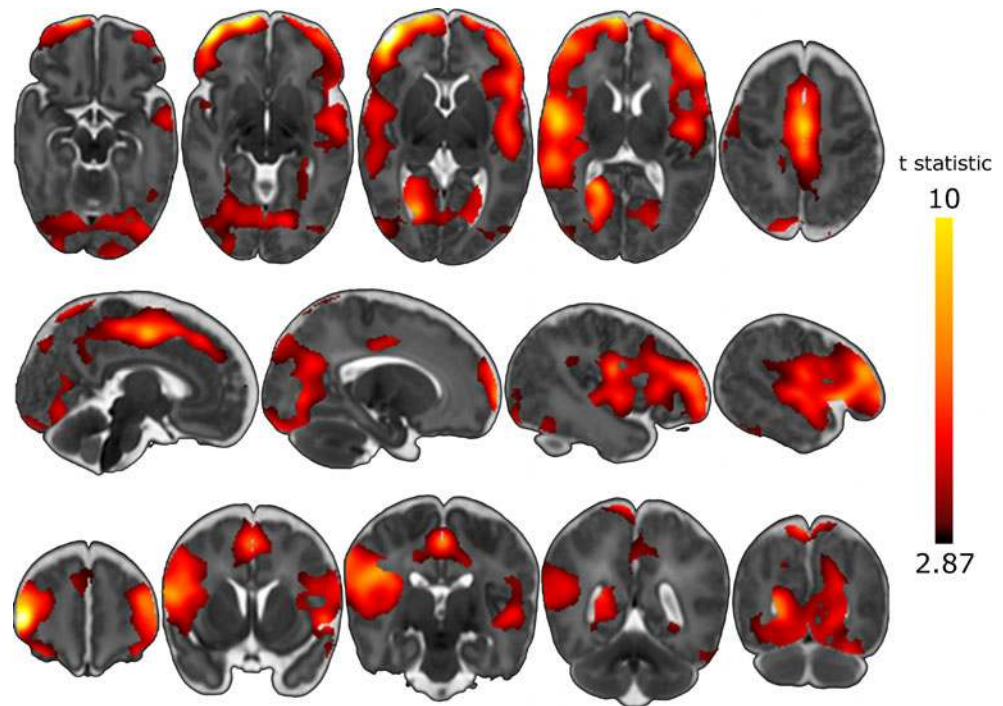
Table 1 (continued)

Author	Demographics	Additional PT criteria	Scanning Details	d-MRI analysis	Neurological outcome(s)	Key findings
	PT: $n=56$, GA at birth=30.1 weeks (23.4–34.1), BW=1,324 g (565–2,120), auditory assessment at median 30 days after term	catchment area, 59 % of PT ($n=56$) had normal conventional MRI, 11 % had minor abnormalities, and 30 % had major abnormalities	1.5 T, 15 days, $b=600$, slice thickness		evoked potentials	correlated with $\uparrow FA$ of the inferior colliculus

Text in italics indicates associations between diffusion parameters and functional outcome or perinatal co-morbidities. 'Controls' refer to term-born controls. GA (gestational age) at birth, BW (birth weight) and scanning age are taken as the mean unless stated otherwise

White matter tracts and structures: *AC* anterior commissure, *ACR* anterior corona radiata, *AF* arcuate fasciculus, *ALIC* anterior limb of the internal capsule, *ATR* anterior thalamic radiations, *CBT* cortico-bulbar tract, *CC* corpus callosum, *CSO* centrum semi-ovale, *CST* cortico-spinal tract, *EC* external capsule, *Fmni* forceps minor, *Fmni* forceps minor, *FOF* inferior fronto-occipito fasciculus, *ILF* inferior longitudinal fasciculus, *OFC* orbito-frontal cortex, *OR* optic radiations, *PLIC* posterior limb of the internal capsule, *PTR* posterior thalamic radiations, *SCR* superior corona radiate, *SLF* superior longitudinal fasciculus, *SS* sagittal striatum, *STR* superior thalamic radiations, *UC* uncinate fasciculus; **Neurocognitive tests:** *ABC* Bayley's Scales of Infant Development, *CELF* Clinical Evaluation of Language Fundamentals, *CGAS* Children's Global Assessment Scale, *COWAT* Controlled Oral Word Association Test, *CTPP* Comprehensive Test of Phonological Processing, *CVLT* California Verbal Learning Test, *DS* Digit Span test, *GDS*, *GMDs* Griffiths Developmental Scale, *GFTA* Goldman-Fristoe Test of Articulation, *GP* Grooved Pegboard test, *HST* Hayling Sentence Completion Test, *ITSEA* Infant Toddler Social Emotional Assessment, *KSADS* Schedule for Affective Disorders and Schizophrenia for School-age Children, *MDI* Mental Developmental Index, *PDI* Psychomotor Developmental Index, *PPVT* Peabody Picture Vocabulary Test, *SCAN-4* Auditory Processing Disorders in Adolescents and Adults, *SDQ* Strengths and Difficulties Questionnaire, *TROG* Test for Reception of Grammar, *VF* Verbal Fluency, *VMI* Visuo-motor Integration, *WASI* Wechsler Abbreviated Scale of Intelligence, *WISC* Wechsler Intelligence Scale for Children, *WJ* Woodcock-Johnson, *WMSI* Wechsler Memory Scale, *WORD* Wechsler Objective Reading Dimensions; **Associated conditions:** *ALD* acute lung disease, *CLD* chronic lung disease, *CP* cerebral palsy, *ROP* retinopathy of prematurity, *VM* ventriculomegaly; **Demographics:** *ADC* apparent diffusion coefficient, *DEHSI* diffuse excessive high signal intensity, *FA* fractional anisotropy, *GA* gestational age, *PT* preterm(s), *TEA* term-equivalent age, *VLBW* very low birth weight, *WMA* white matter abnormalities, *WMSA* white matter signal abnormalities; **d-MRI analysis method:** *IBM* voxel-based morphometry, *TBSS* tract-based spatial statistics, *cUS* cranial ultrasound, *ROI*=region of interest

Fig. 4 Thalamocortical connectivity is significantly reduced in preterm infants. Regions of significantly lower thalamocortical connectivity in preterm infants at term-equivalent age, compared to term-born controls, are shown. Statistical images are displayed on a population-based T₂-weighted template and are corrected for multiple comparisons at $p < 0.001$ FDR-corrected (colour bar indicates t -statistic). Reproduced from [156]



premature newborns with abnormal conventional MRI showed a diminished rate of increasing FA as compared to those with normal imaging [38]. This reduced rate was principally due to changes in λ_{\perp} and was negatively affected by the presence of postnatal infection.

Effect of prematurity from infancy to adulthood

d-MRI studies that assess the effect of prematurity in infancy and childhood are outlined in Table 2. These studies affirm some of the WM microstructural changes detected around birth. Preterm-born infants with corpus callosal thinning show significant reductions in FA in the posterior CC, PLIC and CSO at 1 year, in the genu of the CC and CSO at 2 years and in the genu, isthmus and splenium of the CC at 3 years compared with term-born infants of matching ages [89, 90]. Several studies in this age group suggest that the effects of prematurity are more extensive. Yung et al. showed significantly lower whole-brain FA in a VBM study in healthy preterm children as compared to term-born controls [51], whilst an ROI and tractography-based study in young preterm children with confirmed PVL, found FA reductions across a range of commissural, projection and association tracts [91]. Similarly, a whole-brain tractography approach in children between 1 and 3 years, suggested that prematurity affects anisotropy in tracts connecting all cortical lobes and several sub-cortical structures after accounting for age at imaging [92] (Fig. 5). Differences between the above studies may possibly be due to variation in the study populations and sensitivity of the analyses.

d-MRI studies that assess the effect of prematurity in adolescence are outlined in Table 3. Widespread preterm-associated white matter changes are readily demonstrated at this age. Indeed, preterm born adolescents show reductions in FA; encompassing tracts such as the genu and splenium of the CC, ALIC, PLIC, inferior fronto-occipito fasciculus (IFOF), uncinate fasciculi, superior longitudinal fasciculus (SLF), inferior longitudinal fasciculus (ILF), cingulum bundle, EC, CSO and precentral and frontal subcortical white matter as compared to term-born controls [93–96]. However, pervasive FA reductions may not reflect the broader preterm-born adolescent population as preterm subjects in these studies showed diverse neurological impairment. A recent TBSS study in *normal functioning* preterms found no significant FA reductions, but actually revealed widespread increases in FA [97]. Increases may be artefactual, due to compensatory changes needed in order to maintain normal neurological function [96], or represent a relative increase due to reduction in WM volume, crossing fibres or dendritic branching [97].

There are a limited number of reports which perform diffusion MRI in preterm-born adults (Table 4). Despite examining cohorts of similar ages, they apply differing methodologies, yet confirm that WM microstructural changes are persistent in adulthood. Kontis et al. compared microstructural values in the corpus callosum in preterm and term-born adults using diffusion tractography and observed significant differences in MD in the genu and whole CC between preterm and term-born females [98]. Applying a whole-brain VBM approach, Allin et al. [99] demonstrated FA reductions in the CC, bilateral SLF and SCR in a VLBW preterm-born adult

Table 2 d-MRI studies of preterms in infancy or during childhood

Author	Demographics	Additional PT criteria	Scanning details	d-MRI analysis	Neurological outcome(s)	Key findings
Pandit et al. 2013 [92]	PT: $n=49$, median GA at birth=28.3 weeks (24.6–34.7), median BW=986 g (560–3,710), median corrected scan age=13 months (11–31), 7 subjects with paired imaging	Exclusion criteria: focal, macrostructural lesions on conventional MRI including cystic PVL, HPI or posthaemorrhagic VM. At term, 10.4 % PT had GMH, 8.3 % had punctate WM lesions and 2 % had moderate VM	3 T, 32 days, $b=750$, slice thickness=2 mm	Tractography (whole-brain probabilistic)	–	↑ GA was associated with ↑ FA in widespread, bilateral connections linking cortical and subcortical structures. - These include commissural, projection and association fibres
Lee et al. 2012 [89]	PT: $n=18$, GA at birth=30.3 weeks (26.3–35.7), BW=1,520 g (900–2,600), corrected scan age=14.9 months (1–35), CC thinning Controls: $n=18$, GA at birth=39.4 weeks (38.1–41.7), BW=3,056 g (2,800–3,520), corrected scan age=14.6 m (1–36)	Inclusion criteria: <37 weeks GA at birth, no definite evidence of a focal lesion except CC thinning by conventional MRI, the absence of any diagnosed genetic syndrome or seizure, epilepsy, no history of trauma or brain surgery	1.5 T, 32 days, $b=1,000$, slice thickness=2 mm	TBSS	–	Between infants <12 months, ↓ FA in PT sub-group in bilateral CSO, IC, EC, Fornix, CP, ILF, IFOF, CC genu and splenium compared to control sub-group. - Between children 12–24 months, ↓ FA in PT in similar regions as previous but reduced globally and between 24 and 36 months, ↓ FA in PT sub-group only in CSO and CC genu. - Maturation changes (↑ FA) were significant up to 24 months in normal controls but continued until 36 months in PT
Wang et al. 2012 [91]	PT: $n=46$, GA at birth=32.5 weeks, scan age=16 months (3–36 months) Controls: $n=16$, scan age=16 months (3.5–36)	All PT had confirmed CP and PVL	3 T, 15 days, $b=800$, slice thickness=3 mm	ROI, Tractography (Deterministic)	Gesell Development Scale (Chinese adaptation)	PT group showed ↓ FA in bilateral CST, ALIC, PLIC, AF, CR, SLF, ATR, CC splenium. ↓ FA was associated with worse cognitive level in association fibres: bilateral AF, CG, SLF; projection fibres: bilateral PLIC, ALIC, PTR, CR, CP and left CST and commissural fibres: CC genu and splenium
Jo et al. 2012 [90]	PT: $n=22$, GA at birth=31.4 weeks (26.1–35.7),	Inclusion criteria: <37 weeks GA at birth, no definite evidence of a focal lesion except CC thinning by conventional MRI, the absence of any diagnosed	1.5 T, 32 days, $b=600$, slice thickness=2.3 mm	ROI, Tractography (Deterministic)	–	PT group had ↓ voxel count and ↓ FA in the CC, particularly the isthmus.

Table 2 (continued)

Author	Demographics	Additional PT criteria	Scanning details	d-MRI analysis	Neurological outcome(s)	Key findings
	BW=1,700 g (1,000–3,000 g), corrected scan age=36 months (6–60). Follow up scan for <i>n</i> =11 at 46.8 months (19–71) Controls: <i>n</i> =23, corrected scan age=34.5 months (4–60). Follow up scan for <i>n</i> =11 at 46.7 months (18–73)	genetic syndrome or seizure, epilepsy, no history of trauma or brain surgery.				Incremental maturational changes (↑ FA in CC) were smaller in PT group. For WM tracts passing through CC, PT group displayed ↓ FA, streamline count and ↑ ADC compared to controls.
Andrews et al. 2009 [165]	PT: <i>n</i> =19, GA at birth=30.5 weeks (24–36), BW=1,455 g (572–2,608), scanning age=11.9 years Controls: <i>n</i> =9, BW=3,877 g (2,863–4,423)=12.7 years	68 % PT with normal conventional MRI, 32 % with mild–moderate abnormalities. 5 % PT had CP	3 T, 6 days, <i>b</i> =850, slice thickness=4 mm	ROI	WASI, WJ-III: word identification, word attack, passage comprehension	PT group showed ↓ FA in the total CC and in splenium, body and genu sections. - ↑ BW associated with ↑ FA in CC and temporo-parietal WM. - ↑ FA in CC body associated with ↑ word identification
Counsell et al. 2008 [112]	PT: <i>n</i> =33, median GA at birth=28.7 weeks (24.6–32.1), median BW=1,080 g (745–1,940), scanning age=25.5 months (24–27)	Inclusion criteria: PT <32 weeks GA. Exclusion criteria: congenital or chromosomal abnormalities, congenital infection, post-haemorrhagic hydrocephalus, HPI, cystic PVL, post-haemorrhagic VM on neonatal MRI	3 T, 15 days, <i>b</i> =750, slice thickness=2 mm	TBSS	GMDS	↑ DQ associated with ↑ FA in the CC. - ↑ Performance subscales associated with ↑ FA in the CC and right cingulum. - ↑ Eye-hand co-ordination associated with ↑ FA in the cingulum, fornix, AC, CC and right UF
Yung et al. 2007 [51]	PT: <i>n</i> =25, GA at birth=29.4, BW=1,141.6, scanning age=10.1 years (8.8–11.5), IQ assessment at 6 months after imaging Controls: <i>n</i> =13, scanning age=10.1 years (8.5–12.5)	Inclusion criteria: PT <37 weeks GA, BW <1,500 g, good health besides prematurity, neurological exam normal. 12 % PT had mild conventional MRI abnormality	1.5 T, 25 days, <i>b</i> =1,200, slice thickness=5 mm	VBM	WISC	↓ whole-brain WM volume and FA in PT compared to controls. - ↑ IQ associated with whole-brain WM volume and FA
PL Khong et al. 2006 [111]	PT: <i>n</i> =22, GA at birth=28.3 weeks (24–34), BW=1,110.2 g (650–1,475), scanning	Inclusion criteria: PT <37 weeks GA and BW <1,500 g. Exclusion criteria: congenital malformations or VM on conventional MRI, CP	1.5 T, 25 days, <i>b</i> =1,200, slice thickness=5 mm	VBM	WISC	↑ FA in bilateral occipito-temporal, temporo-parietal and frontal WM was associated with IQ

Table 2 (continued)

Author	Demographics	Additional PT criteria	Scanning details	d-MRI analysis	Neurological outcome(s)	Key findings
Nagy et al. 2003 [135]	age=10.2 years (9.2–11.5) PT: <i>n</i> =9, GA at birth=28.6 weeks, BW=1,098 g, scanning age=10.9 years. Controls: <i>n</i> =10, scanning age=10.8 years	Inclusion criteria: preterm children with motor/distractibility scores >2 SD above population mean. Exclusion criteria: cystic PVL or IVH on cUS, IQ<80 at 57. All PT had attention deficits	1.5 T, 20 days, <i>b</i> =1,000, slice thickness=5 mm	VBM	–	PT group showed ↓ FA in the bilateral posterior CC and bilateral IC

White matter tracts and structures: *AC* anterior commissure, *ACR* anterior corona radiata, *AF* arcuate fasciculus, *ALIC* anterior limb of the internal capsule, *ATR* anterior thalamic radiations, *CBT* cortico-bulbar tract, *CC* corpus callosum, *CSO* centrum semi-ovale, *CST* cortico-spinal tract, *EC* external capsule, *Fmaj* forceps minor, *IFOF* inferior fronto-occipito fasciculus, *ILF* inferior longitudinal fasciculus, *OFC* orbito-frontal cortex, *OR* optic radiations, *PLIC* posterior limb of the internal capsule, *PTR* posterior thalamic radiations, *SCR* superior corona radiata, *SLF* superior longitudinal fasciculus, *SS* sagittal striatum, *STR* superior thalamic radiations, *UC* uncinate fasciculus; **Neurocognitive tests:** *ABC* Movement Assessment Battery for Children, *ADHD_RS* Attention Deficit/Hyperactivity Disorder Rating Scale, *ASSQ* Autism Spectrum Screening Questionnaire, *BSD* Bayleys Scales of Development, *CELF* Clinical Evaluation of Language Fundamentals, *CGAS* Children's Global Assessment Scale, *COVAT* Controlled Oral Word Association Test, *CTPP* Comprehensive Test of Phonological Processing, *CVLT* California Verbal Learning Test, *DS* Digit Span test, *GDS*, *GMDS* Griffiths Developmental Scale, *GFTA* Goldman Frisbee Test of Articulation, *GP* Grooved Pegboard test, *HSCIT* Hayling Sentence Completion Test, *ITSEA* Infant Toddler Social Emotional Assessment, *KSADS* Schedule for Affective Disorders and Schizophrenia for School-age Children, *MDI* Mental Developmental Index, *PDI* Psychomotor Developmental Index, *PPVT* Peabody Picture Vocabulary Test, *SCAN-A* Auditory Processing Disorders in Adolescents and Adults, *SDQ* Strengths and Difficulties Questionnaire, *TROG* Test for Reception Of Grammar, *VF* Verbal Fluency, *VMI* Visuo-motor Integration, *WASI* Wechsler Abbreviated Scale of Intelligence, *WCST* Wisconsin Card Sorting Test, *WISC* Wechsler Intelligence Scale for Children, *WJ* Woodcock-Johnson, *WMSI* Wechsler Memory Scale, *WORD* Wechsler Objective Reading Dimensions; **Associated conditions:** *ALD* acute lung disease, *CLD* chronic lung disease, *CP* cerebral palsy, *ROP* retinopathy of prematurity, *VM* ventriculomegaly; **Demographics:** *ADC* apparent diffusion coefficient, *DEHSI* diffuse excessive high signal intensity, *FA* fractional anisotropy, *GA* gestational age, *PT* preterm(s), *TEA* term-equivalent age, *VLBW* very low birth weight, *WMA* white matter abnormalities, *WMSA* white matter signal abnormalities; **d-MRI analysis method:** *VBM* voxel-based morphometry, *TBSS* tract-based spatial statistics, *cUS* cranial ultrasound, *ROI*=region of interest

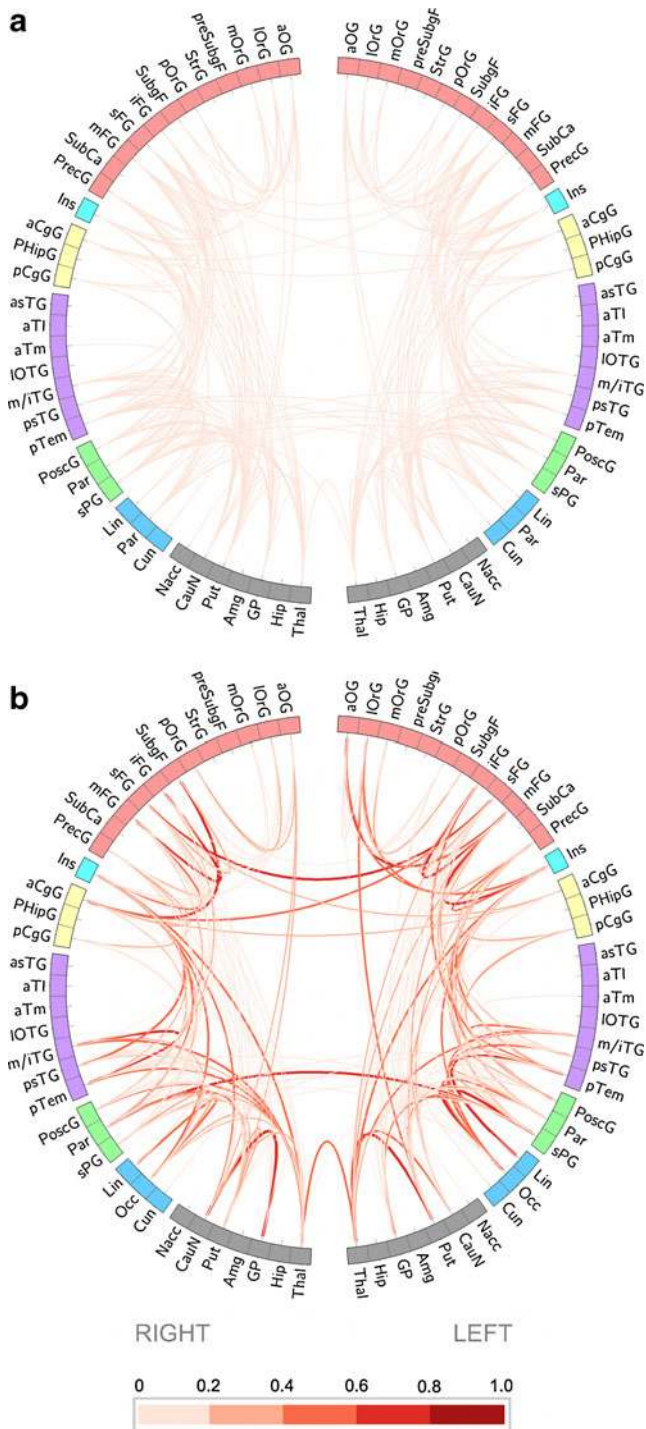


Fig. 5 Effect of prematurity on whole-brain structural connectivity in childhood. Connections are unweighted (a) or weighted according to their predictive importance with respect to post-conceptual age at birth (prematurity, b). Increased thickness and coloration of lines (legend) indicates higher selection probability of connections being in the predictive model. Regions of interest (ROIs) are divided in blocks according to lobe (red: frontal, cyan: insula, yellow: limbic, purple: temporal, green: parietal, blue: occipital, grey: subcortical structures) and shown in relative anatomical location (anterior and posterior correspond to the top and bottom of each connectogram). Reproduced from [92]. A full list of abbreviations for individual ROIs are provided in [92]

group as compared to term-born controls. In this study, GA was shown to be positively associated with FA in the right SLF, whilst birth weight was positively related with the body and splenium of the CC and bilateral SLF. This report also noted increased FA in preterms in several tracts including bilateral IFOF, UF, ACR (which were all negatively correlated with GA) and the SLF. In contrast to Allin and colleagues, Eikenes et al. [100] explored whole-brain diffusion changes using TBSS and noted more widespread effects of prematurity, in line with the evidence from adolescent studies [100]. Reduced FA in very low birth weight (VLBW) preterm-adults was found in the cerebellar peduncles, CST, CPT, superior and posterior CR, UF, SLF, ILF, IFOF, cingulum, posterior thalamic radiations (PTR), fornix, thalamus, CC, EC and stria terminalis on both sides. These extensive reductions were principally due to the increase in the second and third eigenvalues and were maintained after removal of subjects with CP. Similar to the previous study, areas with increased FA were also found and these included the superior CR, CST, CPT and superior TR on the right side.

In summary, the impact of premature birth on cerebral WM is significant and observable across all stages of life: from TEA through to adulthood. The presented studies vary widely in methodology but largely affirm WM anisotropy reductions in preterm-born individuals.

Relationship between diffusion MRI and neurological function

Neurological function and dysfunction are related to variations in WM microstructure [101]. The disruption of WM connections and associated structures following WMI likely underly the neurological impairments observed after preterm birth. In the next section, we aim to chart the relationship between d-MRI markers and neurodevelopmental outcome in preterm-born individuals across the lifespan. We collate studies which explore structure–function associations in preterms, and focus on five key domains known to be affected by preterm birth: neurosensory ability, cognition, language, motor ability and behaviour.

Neurosensory ability

Although now less common, neurosensory impairments involving vision or hearing still continue to affect individuals born preterm [4]. Several studies have associated visual performance with FA in the OR of premature neonates [102–105]. Glass et al. [104] performed diffusion tractography in a small sample of normal functioning, late preterm neonates shortly after birth and then tested their visual-evoked response amplitudes in early infancy. Peak response amplitudes for

Table 3 d-MRI studies of preterms during adolescence

Author	Demographics	Additional PT criteria	Scanning details	d-MRI analysis	Neurological outcome(s)	Key findings
Northam et al. 2012 [125]	PT: <i>n</i> =50, GA at birth=27.5 weeks, scan age=16 years Controls: <i>n</i> =30, scan age=age-matched	Exclusion criteria: incomplete records. At birth, 56 % of PT final cohort had positive eUS findings and 54 % had abnormal findings on conventional MRI (PVWM reduction or reduced CC size). 8 % of PT with CP, 6 % with neurosensory deficit, 24 % with minor neurology findings	60 days, <i>b</i> =3,000, slice thickness=3 mm	ROI	WASI, GFTA, CTPP	PT group divided into those with and without focal oromotor control (FOC) impairment. - ↓ FA in CST/CBT in FOC-impaired PT group, with hemisphere-by-group interaction effect due to ↓ FA in left more than right PLIC. - FOC impairments predicted by left motor tract FA
Feldman et al. 2012 [121]	PT: <i>n</i> =23, GA at birth=28.7 weeks, scan age=12.5 years	Inclusion criteria: ≤6 weeks GA and BW <2,500 g. Exclusion criteria: seizure disorder; VM, hydrocephalus, receptive vocabulary score <70, sensorineural hearing loss, or were a non-English speaker. 17 % PT at birth had abnormal cUS or MRI and 9 % with mildly abnormal findings. At scanning age, 39 % had mild abnormal findings on TI	3 T, 30 days, <i>b</i> =900, slice thickness=2 mm	TBSS, ROI	WASI, CELF-4, PPVT-III, TROG-2, WJ-III	In PT group, FA in a wide bilateral WM skeleton was associated with several reading and language measures. - ROIs where FA was associated with outcome after multiple linear regression: right IFOF and verbal IQ and syntactic comprehension; forceps minor with receptive vocabulary and verbal memory; right ATR and linguistic processing speed; CC genu and decoding, left UF and reading comprehension
Northam et al. 2012 [122]	PT: <i>n</i> =50, GA at birth=27 weeks, scan age=16 years Controls: <i>n</i> =30, scan age=age-matched	At birth, 56 % PT had positive cUS findings and 54 % had abnormal findings on conventional MRI (PVWM reduction or reduced CC size).	1.5 T, 60 days (HARDI), <i>b</i> =3,000, slice thickness=3 mm	Tractography (CSD - Probabilistic), TBSS, VBM	WASI, CELF-3, EROWPV, WORD, CTOPP, DS, SCAN-A, SDQ, GDS	19 (38 %) PT labelled language impaired (LI) as 1.5 SD lower than mean CELF score of controls. - VBM and TBSS showed ↓ FA in posterior CC and temporal WM in LI vs. normal PT. - right direct AF, UF, (posterior) CC volume in LI vs. normal PT. - AC size and volume of temporal lobe intrahemispheric fibres predict LI
Feldman et al. 2012 [97]	PT: <i>n</i> =58, GA at birth=29.4 weeks, scan age=12.6 years (site 1, <i>n</i> =25; site 2, <i>n</i> =33) Controls: <i>n</i> =63, GA at birth=<37 weeks, scan age=12.9 years	Inclusion criteria: <36 weeks GA. Exclusion criteria: active seizures, complications of ventriculoperitoneal shunt for hydrocephalus, moderate to severe VM, congenital malformation, meningitis or encephalitis; receptive vocabulary score <70; sensory	Site 1: 3 T, 30 days, <i>b</i> =900, slice thickness=2 mm; Site 2: 3 T, 6 days, <i>b</i> =850	TBSS	WASI	PT were high functioning with average IQ. - No WM areas where FA was lower in PT than controls in either site. - Multiple areas where FA was higher in PT at site 1 and axial diffusivity was higher in site 2. - ↓ FA in CC and posterior PVWM associated with ↑ WMI score at both sites. - ↑ FA associated with ↑ IQ in PT group at site 1 in bilateral ATR, CST, SLF, UF, left CG and Fmin and right IFOF

Table 3 (continued)

Author	Demographics	Additional PT criteria	Scanning details	d-MRI analysis	Neurological outcome(s)	Key findings
Lindqvist et al. 2011 [106]	(site 1, $n=40$; site 2, $n=23$) PT: VLBW, $n=30$, GA at birth=29.3 weeks (24–35), scan age=15.1 years (14.1–16.9), eye assessment age=14.5 years (13.6–15.4) Controls: $n=45$, GA at birth=39.5 weeks (37–42), scan age=15.3 years (14.2–16.4) eye assessment age=14.6 years (13.6–16.8)	impairments; and non-English speaker. At birth, 32 % of PT at site 1 had abnormal cUS or MRI, at site 2 15 % PT had abnormal cUS or MRI. Exclusion criteria: chromosomal abnormality present. 13 % PT had mild–moderate CP. PT with known brain lesions not excluded.	1.5 T, 6 days, $b=1,000$, slice thickness=5 mm	VBM, ROI	Visual acuity, convergence, stereopsis, contrast sensitivity and strabismus	\uparrow FA, \downarrow λ , associated with \uparrow acuity scores in CC splenium, midbody and frontal WM
Mullen et al. 2011 [96]	PT: $n=44$, GA at birth=28.3 weeks, scan age=16.4 years Controls: $n=41$, scan age=16.3 years	Exclusion criteria: IVH, PVL, VM. All PT had normal conventional MRI and total ventricular volume within 2 SD of the mean term ventricular volume. Inclusion criteria: $BW \leq 1,500$ g	1.5 T, 32 days, $b=1,000$, slice thickness=3 mm	VBM, ROI, Tractography (Deterministic)	WISC, PPVT, CTTP	PT group had lower full, verbal and performance IQ scores and phonemic awareness. - PT had \downarrow GM, WM and total tissue volume; \downarrow FA in bilateral UF, EC, IFG, CC genu and splenium as vs. controls. - In PT group, \uparrow FA in bilateral AF associated with CTOPP; left UF with PPVT
Skranes et al. 2009 [114]	PT: VLBW, $n=34$, GA at birth=29.3 weeks, scan age=15.2 years		1.5 T, 6 days, $b=1,000$	VBM	WCST-III	\uparrow FA in left CG and bilateral IFOF were associated with \uparrow WCST score
Constable et al. 2008 [95]	PT: $n=29$, GA at birth=28.4 weeks, BW=974 g, scan age=12.2 years Controls: $n=22$, scan age=12.5 years	Exclusion criteria: IVH, PVL, VM, abnormal neurological findings, ventricular volume within 2 SD of mean term ventricular volume and neonatal cUS evidence of IVH, WMI and VM	1.5 T, 6 days, $b=1,000$, slice thickness=3 mm	ROI, VBM, Tractography (Deterministic)	WISC, PPVT, VMI	PT had \downarrow full, verbal and performance IQ and VMI vs. controls. - PT had \downarrow temporal and deep GM volume and \downarrow bilateral frontal, temporal, parietal and deep WM. - PT had \downarrow FA in bilateral anterior UF, anterior IFOF, right posterior IFOF, left SFOF, EC, CC splenium and CG; and in the subcortical WM: bilateral precentral gyri, right STG and Fmaj
Skranes et al. 2007 [94]	PT: $n=34$, GA at birth=29.3 weeks, BW=1,218 g, scan age=15.2 years	Exclusion criteria: chromosomal abnormality present. Inclusion criteria: $BW \leq 1,500$ g. 12 % of PT had CP	1.5 T, 6 days, $b=1,000$, slice thickness=5 mm	VBM	VMI-IV, WISC-III, GP, Movement	PT had \downarrow FA and \uparrow λ_{11} in bilateral ALIC, PLIC, EC, CC genu and splenium, ILF, SLF. In the PT group, \uparrow FA in the EC was associated with \uparrow VMI scores, visual perception scores with EC and PLIC, motor coordination scores with right SLF and left

Table 3 (continued)

Author	Demographics	Additional PT criteria	Scanning details	d-MRI analysis	Neurological outcome(s)	Key findings
Vangberg et al. 2006 [93]	<p>Controls: $n=47$, GA at birth=39.5 weeks, BW=3,670 g, scan age=15.5 years</p> <p>PT: $n=34$, GA at birth=29.3 weeks, BW=1,218 g, scan age=15.2 years; SGA: $n=42$, GA at birth=39.2 weeks, BW=2,902 g, scan age=15.6 years</p> <p>Controls: $n=47$, GA at birth=39.5 weeks, BW=3,670 g, scan age=15.5 years</p>	<p>Inclusion criteria: BW $\leq 1,500$ g.</p> <p>Exclusion criteria: chromosomal abnormality present.</p> <p>15 % of PT had CP</p>	<p>1.5 T, 6 days, $b=1,000$, slice thickness=5 mm</p> <p>VBM</p>	–	<p>ABC, KSADS, ASSO, ADHD-IV, CGAS</p>	<p>middle fasciculus, performance IQ scores with right PLIC, verbal IQ with right SLF. - Fine motor impairments were related to \downarrow FA in the ALIC, PLIC and SLF. - Low CGAS score associated with \downarrow FA in IC, EC and long fascicles. - ADHD children had low FA in several areas with strongest associations in the EC and the inferior and middle long fascicles on the left.</p> <p>PT vs. controls: \downarrow FA in PLIC, CSO, PVWM (SLF) and CC, mainly due to $\uparrow \lambda_{\text{iso}}$; limited voxels with \uparrow FA in brainstem and left CSO</p>

White matter tracts and structures: AC anterior commissure, ACR anterior corona radiata, AF arcuate fasciculus, ALIC anterior limb of the internal capsule, ATR anterior thalamic radiations, CBT cortico-bulbar tract, CC corpus callosum, CSO centrum semi-ovale, CST cortico-spinal tract, EC external capsule, Fmaji forceps minor, Fmif forceps minor, IFOF inferior fronto-occipito fasciculus, ILF inferior longitudinal fasciculus, OFC orbito-frontal cortex, OR optic radiations, PLIC posterior limb of the internal capsule, PTR posterior thalamic radiations, SCR superior corona radiata, SLF superior longitudinal fasciculus, SS sagittal striatum, STR superior thalamic radiations, UC uncinata fasciculus; **Neurocognitive tests:** ABC Movement Assessment Battery for Children, ADHD_RS Attention Deficit/Hyperactivity Disorder Rating Scale, ASSQ Autism Spectrum Screening Questionnaire, BSD Bayleys Scales of Development, CELF Clinical Evaluation of Language Fundamentals, CGAS Children's Global Assessment Scale, COWAT Controlled Oral Word Association Test, CTPP Comprehensive Test of Articulation, GP Grooved Pegboard test, HSCT Hayling Sentence Completion Test, ITSEA Infant Toddler Social Emotional Assessment, KSADS Schedule for Affective Disorders and Schizophrenia for School-age Children, MDI Mental Developmental Index, PDI Psychomotor Developmental Index, PPT Peabody Picture Vocabulary Test, SCAN-A Auditory Processing Disorders in Adolescents and Adults, SDQ Strengths and Difficulties Questionnaire, TROG Test for Reception of Grammar, VF Verbal Fluency, VMI Visuo-motor Integration, WASI Wechsler Abbreviated Scale of Intelligence, WISC Wisconsin Card Sorting Test, WISC Wechsler Intelligence Scale for Children, WJ Woodcock-Johnson, WMSI Wechsler Memory Scale, WORD Wechsler Objective Reading Dimensions; **Associated conditions:** ALD acute lung disease, CLD chronic lung disease, CP cerebral palsy, ROP retinopathy of prematurity, VM ventriculomegaly; **Demographics:** ADC apparent diffusion coefficient, DEHSI diffuse excessive high signal intensity, FA fractional anisotropy, GA gestational age, PT preterm(s), TEA term-equivalent age, VLBIW very low birth weight, WMA white matter abnormalities, WMSA white matter signal abnormalities; **d-MRI analysis method:** VBM voxel-based morphometry, TBSS tract-based spatial statistics, cUS cranial ultrasound, ROI=region of interest

Table 4 d-MRI studies of preterms in adulthood

Author	Demographics	Additional PT Criteria	Scanning Details	d-MRI Analysis	Neurological Outcome(s)	Key Findings
Kontis et al. 2009 [98]	VPT: n=61, scan age=19.1 years (17–22) Controls: n=45, scan age=18.6 years (17–22)	–	1.5 T, 64 days, b=1,300, slice thickness=2.5 mm	Tractography (deterministic)	WASI, CVLT	VPT females had higher ADC in total CC and genu than term females - Higher genu ADC associated with lower performance IQ in VPT females - ADC in CC body associated with CVLT intrusions in VPT group - In term group, ADC in CC genu and splenium associated with CVLT-learning slope, ADC in CC body with CVLT false-positive
Allin et al. 2011 [99]	PT: n=80, GA at birth=28.9 weeks, scan age=19.2 years (17–22) Controls: n=41, GA at birth=40.2 weeks, scan age=18.6 years (17–22)	Exclusion criteria: VM, lateral ventricular volume exceeded normal maximum (46 mm ³)	1.5 T, 64 days, b=1,300, slice thickness=2.5 mm	VBM	WASI, COWAT, HSCT, CVLT, WMSI, semantic and phonetic VF	VPT group had ↓ full, verbal, performance IQ; ↓ CVLT, ↓ HSCT, ↓ semantic and phonetic VF scores compared to term - ↓ FA in VPT group in CC, bilateral SLF, left SCR: these clusters associated with ↑ performance IQ, CVLT - ↑ FA in VPT group in bilateral IFOF, UF, SLF, ACR - ↑ GA associated with ↑ FA in right SLF and with ↓ FA in bilateral IFOF, UF, ACR - ↑ BW associated with ↑ FA bilateral SLF, body and splenium of CC
Eikenes et al. 2011 [100]	PT: n=49 (3 with CP), VLBW, GA at birth=29.2 weeks (24–35), scan age=20.2 weeks (18.9–22.1) Controls: n=59, GA at birth=39.7 weeks, scan age=20.3 years (19–21.3)	Exclusion criteria: severe CP and Down's syndrome as inability to perform cognitive assessment	1.5 T, 12 days, b=1,000, slice thickness=2.2 mm	TBSS	WASI	Compared to controls, PT group had ↓ FA and ↑ ADC in bilateral cerebellar peduncles, CST, CPT, SCR, PCR, UF, SLF, IFOF, ILF, cingulum, PTR, fornix, thalamus, CC, EC, ST mainly due to ↑ in λ2 and λ3 diffusivity; and ↑ FA in right SLF - Excluding CP preterms less areas with ↓ FA; areas with ↑ FA increased to right SCR, CST, CPT and STR - ↑ no. ventilator days and days in NICU associated with ↓ FA and ↑ ADC in major central WM tracts - ↑ ADC associated with GA in major central WM tracts - ↑ IQ in PT associated with ↑ FA in major central and peripheral tracts and ↓ ADC in the CC, UF, IFOF, ILF and SLF

White matter tracts and structures: AC anterior commissure, ACR anterior corona radiata, AF arcuate fasciculus, ALIC anterior limb of the internal capsule, ATR anterior thalamic radiations, CBT cortico-bulbar tract, CC corpus callosum, CSO centrum semi-ovale, CST cortico-spinal tract, EC external capsule, Fmij forceps minor, IFOF inferior fronto-occipito fasciculus, ILF inferior longitudinal fasciculus, OFC orbito-frontal cortex, OR optic radiations, PLIC posterior limb of the internal capsule, PTR posterior thalamic radiations, SCR superior corona radiata, SLF superior longitudinal fasciculus, SS sagittal striatum, STR superior thalamic radiations, UC uncinate fasciculus; **Neurocognitive tests:** ABC Movement Assessment Battery for Children, ADHD_RS Attention Deficit/Hyperactivity Disorder Rating Scale, ASSQ Autism Spectrum Screening Questionnaire, BSD Bayleys Scales of Development, CELF Clinical Evaluation of Language Fundamentals, CGLAS Children's Global Assessment Scale, COWAT Controlled Oral Word Association Test, CTPP Comprehensive Test of Phonological Processing, CVLT California Verbal Learning Test, DS Digit Span test, GDS, GMDS Griffiths Developmental Scale, GFTA Goldman Frisioe Test of Articulation, GP Grooved Pegboard test, HSCT Hayling Sentence Completion Test, ITSEA Infant Toddler Social Emotional Assessment, KSADS Schedule for Affective Disorders and Schizophrenia for School-age Children, MDI Mental Developmental Index, PDI Psychomotor Developmental Index, PPTV Peabody Picture Vocabulary Test, SCAN-A Auditory Processing Disorders in Adolescents and Adults, SDQ Strengths and Difficulties Questionnaire, TROG Test for Reception of Grammar, VF Verbal Fluency, VMI Visuo-motor Integration, WASI Wechsler Abbreviated Scale of Intelligence, WCST Wisconsin Card Sorting Test, WISC Wechsler Intelligence Scale for Children, WJ Woodcock-Johnson, WMSI Wechsler Memory Scale, WORD Wechsler Objective Reading Dimensions; **Associated conditions:** ALD acute lung disease, CLD chronic lung disease, CP cerebral palsy, ROP retinopathy of prematurity, VM ventriculomegaly; **Demographics:** ADC apparent diffusion coefficient, DEHSI diffuse excessive high signal intensity, FA fractional anisotropy, GA gestational age, PT preterm(s), TEA term-equivalent age, VLBW <very low birth weight, WMA white matter abnormalities, WMSA white matter signal abnormalities; **d-MRI analysis method:** VBM voxel-based morphometry, TBSS tract-based statistics, cUS cranial ultrasound, ROI=region of interest

spatial frequency sweeps were associated with increasing FA, increasing λ_{\perp} diffusivity and decreasing ADC in the OR. This association was not altered after adjusting for GA, time of imaging or exclusion of infants with detectable WMI on standard imaging [104]. In a study of preterm neonates at TEA, we used probabilistic tractography to examine FA in the OR and assess its relationship with a visual assessment score encompassing a battery of items assessing different aspects of visual ability [102] (Fig. 6). Increasing FA in the OR was associated with better visual assessment score and this correlation was independent of GA at birth, PMA at scan and presence of WM lesions. In addition, a secondary TBSS analysis was performed that confirmed this correlation was isolated to the OR and not mediated via other sub-cortical visual pathways. Associations between FA in the OR and visual ability have been detected in other large sample studies of preterm neonates at term [103, 105]. In the study of Groppo et al. [105], a subset of subjects with serial imaging at birth and at term was also studied. In these subjects we found that visual function was predicted by FA in the OR at term and also by the rate of increase in FA between scans but not by FA at birth [105]. This indicates that microstructural maturation during the late preterm period is necessary for normal visual function in preterm infants. In adolescence, a VBM study found that visual acuity was positively associated with FA and negatively associated with λ_{\perp} in WM areas such as the splenium and midbody of the CC and frontal WM [106].

We identified only one study which related the risk of sensorineural hearing loss to prematurity. In a small cohort of VLBW preterm infants, Reiman et al. evaluated the relationship between microstructure in the inferior colliculus and brain stem auditory-evoked potentials and found that shorter wave latencies (faster transmission) and greater wave amplitude were associated with higher FA values and lower ADC [107].

Cognition

Cognitive functions encompass a number faculties including, but not limited to, executive function, attention and working memory. They are dependent on the efficient communication between several cortical and sub-cortical regions, transmitted over an extensive WM network, embracing inter and intrahemispheric WM connections [108–110]. Predictably, studies of individuals born preterm have indicated that the integrity in a extensive set of WM areas is related to cognitive impairments. Whole-brain approaches in preterm infants identified a positive relationship between FA and IQ in bilateral clusters in the occipito-temporal, temporo-parietal and frontal WM [111] and also across the whole brain [51]. Specific relations between cognition and WM FA in preterm infants were identified in the splenium, whole CC and right cingulum bundle, which were associated with performance IQ and tests of cognitive function [112, 113]. In addition, preterm-born infants with PVL exhibited strong correlations between FA and cognition in the bilateral ALIC, SLF, ACG, PTR, GCC and SCC [91]. In adolescence, Skranes et al. [94, 114] found that arithmetic and block-design IQ subtests were associated with the longitudinal fasciculi and right IC, respectively, and executive function was associated with the left cingulum and bilateral IFOF. Feldman et al. [97] examined two groups of high functioning, adolescent preterms from different sites. In the first group, FA, λ_{\parallel} and ADC were associated with IQ in WM clusters within bilateral projection, association and commissural tracts, but no significant relationship between diffusion parameters and IQ was observed in the second. In a study of VLBW preterm-born adults, positive correlations were observed between FA in central and peripheral WM tracts and total IQ [100]. Negative correlations between MD and IQ were also reported, but were limited to the splenium, body

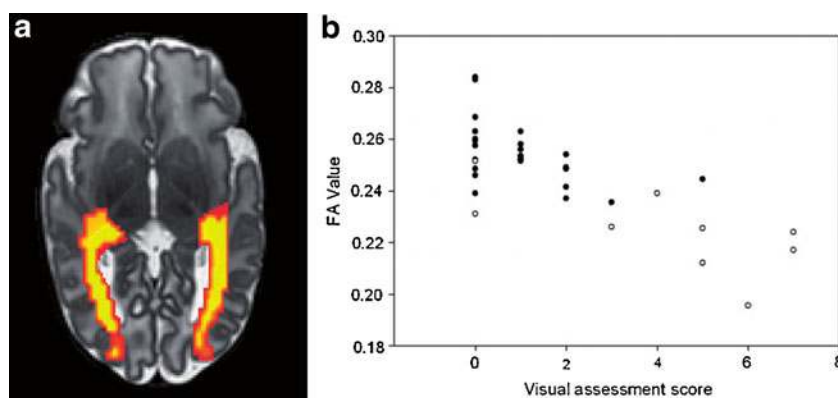


Fig. 6 Fractional anisotropy predicts visual function in preterm neonates. Fractional anisotropy was sampled from the optic radiations (**a**) and was found to be associated with visual assessment score (a low visual assessment score represents good vision) (**b**). The optic radiations were delineated by probabilistic tractography

and are here demonstrated in an infant born at 26 weeks gestational age and imaged at term. In **b**, *black circles* indicate infants with no evidence of abnormality on MRI and *white circles* indicate infants with evidence of focal lesions. Reproduced from [102]

and genu of the CC, UF, IFOF, ILF and SLF. Finally, an adult study that had initially identified FA reductions in the CC, bilateral SLF and left SCR also found that FA in these clusters was positively associated with performance IQ and memory [99]. Despite the heterogeneity within these data, the relationship between cognitive impairments and WM structure shows a predilection for several inter- and intra-hemispheric pathways implicated in cognitive function.

Language

Language encompasses both primary functions, such as the processing of incoming speech and production of meaningful speech output, and secondary functions such as reading and writing [115]. WM tracts that have been implicated in language function in healthy subjects include the ‘dorsal pathway’ or arcuate fasciculus (connecting Wernicke’s and Broca’s area in the left hemisphere) and the ‘ventral pathways’ consisting of the bilateral IFOF, ILF and uncinate fasciculi [116, 117]. There are also other regions thought to be involved in language function such as the corpus callosum [118]. Extensive evidence suggests that structural language correlates are lateralised. Left lateralisation is found in the arcuate fasciculus, and the degree to which this tract is lateralised is associated with language performance [119, 120]. Alterations of diffusion measures in several listed tracts are present in preterm-born subjects, and are related to predictable functional impairments. Several reports have investigated the association between language skills and WM diffusion properties in school-aged children and adolescents born preterm. Advanced language ability was associated with greater FA and this relationship was identified for phonological awareness and the bilateral AF; receptive vocabulary and the left UF and forceps minor; syntactic comprehension and the right IFOF; word identification and the body and genu of the CC; reading comprehension and the left UF; verbal memory and the forceps minor and splenium of the CC; language processing speed and right anterior thalamic radiation (ATR) [94, 96, 121]. Similar to the above associations, Northam et al. found that preterm-adolescents with collective receptive and expressive language impairment, exhibited reduced FA in the posterior CC and temporal WM and reduced tract volumes in the UF, posterior CC temporal connections and the direct segments of the AF as compared to preterms with normal language function [122]. Both anterior commissural (AC) size and the volume of inter-hemispheric temporal lobe connections predicted language impairment, whereas impairment severity was only predicted by AC area. This article also examined the relations of several composite abilities. ‘Complex language’ was positively associated with fibre volume in bilateral UF, AC and splenium of the CC; ‘phonological processing’ with bilateral direct segments of the AF and ‘vocabulary’ was associated with AC size [122]. Like healthy

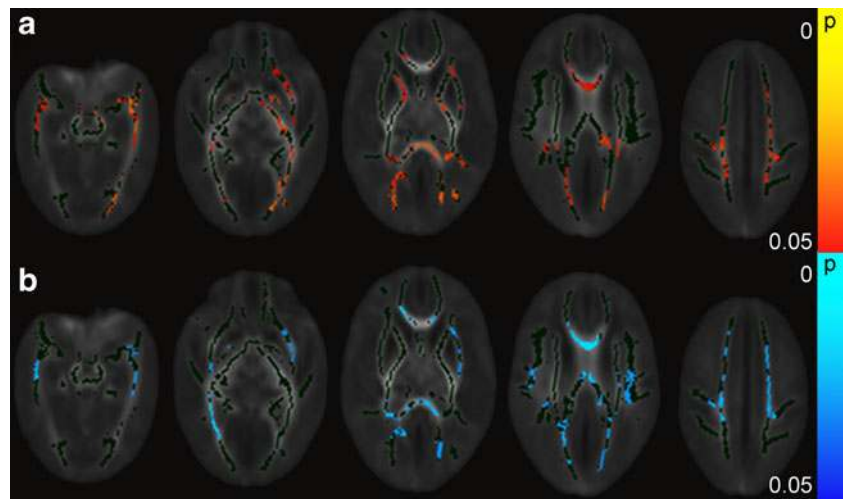
individuals, these findings suggest that the integrity of the classically defined dorsal and ventral pathways are also associated with language function in preterms. However, several departures from the normal model of language architecture are apparent in this population. There is a lack of left-sided lateralisation and increased recruitment of right hemispheric white matter tracts, which are positively associated with ability. This may be indicative of compensatory WM changes [96, 121, 122].

Motor ability

Preterm-born individuals frequently experience adverse motor outcomes [4, 123]. Whilst descending motor pathways such as the CST and PLIC are likely to be affected in preterms, tests of fine motor function also engage cognitive abilities, thus a wider set of WM tracts is also implicated. Three studies imaged preterms at TEA and assessed motor function during infancy and childhood. A TBSS approach found associations between gross or fine motor function and diffusion markers in distributed WM clusters [113]. FA in the left PLIC, thalamus and fornix were positively correlated with gross motor score, whereas λ_{\perp} diffusivity in the PLIC, CC, fornix and posterior cingulum were negatively associated. Fine motor scores were positively correlated with FA in the whole CC, CST, CR, SLF, ILF, IFOF, fornix, EC, right UF and cingulum and negatively associated with λ_{\perp} diffusivity in the right PLIC and left CST. Probabilistic tractography and ROI methods found that increased FA in the PLIC and lower ADC and λ_{\perp} in the splenium of the CC were associated with psychomotor function [40, 124]. Imaging during childhood revealed that eye–hand coordination was correlated with FA values in the AC, CC, right UF, cingulum and fornix [112]. By adolescence, visuo-motor integration was associated with FA in the EC and PLIC and motor co-ordination was correlated with FA in the right superior and left middle fasciculi [94]. Fine motor impairment was associated with FA reductions in the PLIC and superior fasciculi [94] and oro-motor impairment was associated with FA reductions in the CST and cortico-bulbar tract (CBT) [125]. Whilst there appeared to be consistency between motor function and tract integrity in the PLIC and CST, relations between white matter integrity and other measures of motor function were variable. This may be because of differences between motor assessments.

Approximately 10 % of preterm-born infants develop CP and this group makes up 40 % of those with the condition [126]. CP describes a non-progressive, heterogenous group of disorders of movement and posture, occurring in the developing fetal or infant brain [127]. Like other preterm infants with neuromotor morbidity, this group shows a similar distribution of WM microstructural changes. A full appraisal of the use of d-MRI in CP infants is beyond the scope of this paper, however, we refer the reader to a recent review by Scheck

Fig. 7 Respiratory morbidity is associated with altered white matter microstructure in preterm neonates. Using TBSS chronic lung disease was found to be associated with significantly increased λ_{\perp} (**a**) and decreased FA (**b**) but not λ_{\parallel} , independent of both gestational age at birth and postmenstrual age at scan (FWE-corrected, $p < 0.05$; colour bars indicate p value). The mean FA skeleton is shown in dark green. Reproduced from [87]



and colleagues for more detail [128]. Preterm-born subjects with CP display decreased FA and increased MD in motor pathways, principally the CST, and sensory pathways such as the PTR when compared to healthy controls. Diffusion indices in these tracts correlate with measures of sensorimotor function and clinical severity of CP [128]. WMI and posterior cystic PVL lesions underly many of the sensorimotor deficits seen in this group [129].

Behaviour

Individuals born preterm are at an increased risk of psychiatric morbidity. Specific behavioural disorders known to be elevated among preterm children and adolescents include emotional impairments, attention-deficit hyperactivity disorder (ADHD) and autism spectrum disorders (ASD) [130, 131]. Bhutta et al. showed that preterm born children have an increased risk of developing ADHD and also frequently manifest externalising or internalising behaviours during school age [132], whilst Aarmoudse-Moens and colleagues [133] confirmed in a recent meta-analysis, the presence of inattention and internalising behaviour in this group. d-MRI studies which relate WM microstructural alterations with behavioural assessments are limited. In a large prospective study, Rogers et al. examined the relationship between diffusion or volumetric measures at TEA and socio-emotional outcomes at 5 years. Higher ADC in the right orbito-frontal cortex, a region implicated in ASD, was associated with peer-relationship problems in later childhood [134]. In a small sample of preterm children with attention deficits, WM disturbances were detected bilaterally within the IC and posterior CC as compared to term-born controls [135]. A study in adolescents found that performance in several tests of mental health were each associated with FA in distributed WM areas [94]. This is somewhat anticipated, since psychosocial disorders are associated with poor cognition [130], which itself is related to extensive WM damage

(see above). Low FA in the bilateral IC, EC and long fascicles was related to worse overall mental health functioning, and adolescents diagnosed with ADHD had lower FA values; predominantly in the left-sided EC, inferior and middle fascicles. In addition, high autistic spectrum screening scores were correlated with low FA values in the left EC and SF [94].

Perinatal co-morbidities

Perinatal co-morbidities are frequent and have been shown to have a significant impact on the developing brain. In this section, we examine studies which utilise d-MRI in assessing the influence of these diseases on WM. Perinatal infection is recognised as an important risk factor for cerebral WMI and a high proportion of neonates born preterm with a confirmed perinatal infection, suffer neurological impairments at a later age [136]. A large, recent study by Chau and colleagues found that postnatal infection in preterm neonates at TEA, was associated with widespread microstructural WM abnormalities [137]. This relationship persisted in infants with infection without positive culture. Reduced FA, increased ADC and λ_{\perp}

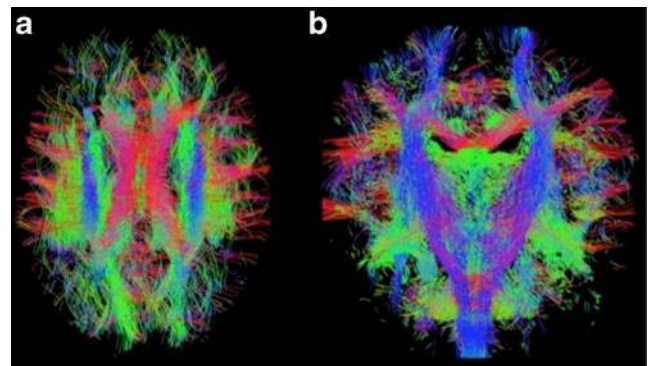


Fig. 8 Whole brain tractography obtained using high angular resolution diffusion imaging (HARDI) and constrained spherical deconvolution (CSD) in a preterm infant at term equivalent age

diffusivity were found in newborns with infection as compared to those without, and the greatest differences occurred in the posterior WM, PLIC and genu of the CC. Postnatal infection was also found to reduce the rate of FA increase in the CST [38]. In contrast to these findings, studies examining chorioamnionitis and coagulase-negative staphylococcal sepsis found no significant interaction with diffusion measures [138, 139].

Respiratory morbidities are also common in the preterm population [4, 140]. We have applied TBSS to investigate effects of respiratory distress in two studies. In the first, acute and chronic lung disease (CLD) were associated with reduced FA in the genu of the CC and the left ILF, respectively [141]. In the second paper, an optimised TBSS protocol for neonates and found that decreased FA in the bilateral CC, CSO, ILF and EC and increased RD in bilateral CC, IC, CSO, ILF and left EC were associated with CLD [142] (Fig. 7). Length of respiratory support was also associated with widespread reductions in FA and increases in λ_{\perp} across the WM skeleton. Differences in result between studies are possibly due to refinements in the method and larger sample size.

Perinatal interventions

There are few studies which have employed d-MRI measures to examine the efficacy of perinatal interventions in preterm infants. Available studies have all employed manually defined ROIs to assess the structural impact of intervention. Very preterm infants who received caffeine treatment showed reduced ADC and λ_{\perp} in several WM regions as compared to a placebo group [143]. These regions lay within the superior occipital and sensorimotor WM and superior and inferior frontal WM. λ_{\parallel} was also significantly reduced within these regions but changes in FA were found to be non-significant. A study from the same group, and using the same anatomical ROIs, found that preterm infants whose parents received an early sensitivity training program showed reduced ADC within the inferior occipital WM, reduced λ_{\perp} in the superior sensorimotor but also reduced λ_{\parallel} in the superior and inferior occipital WM as compared to controls [144]. Als and colleagues applied an environmental intervention in preterm neonates shortly after birth and showed higher relative anisotropy in the left internal capsule and better neurobehavioural functioning in the intervention group as compared to controls [145].

Discussion

Limitations of diffusion MRI literature in the preterm brain

Important limitations impede the interpretation of d-MRI studies. First is the lack of precision in d-MRI metrics and their correlation with neuroanatomical features. Taking the

most commonly used diffusion measure, FA, as an example, it has been shown to relate with several structural features including myelin thickness, membrane integrity, packing density and axonal diameter but also fibre geometry and complexity [101]. As such, there is no one-to-one relationship with any specific microstructural component. In addition, the experimental studies which sought a relation between anisotropy and the underlying neurobiology (see previous) were largely performed in a controlled environment rather than in the complex medium of the developing brain. Thus relating changes in FA in the preterm brain with aspects of WM pathology must be done with caution. λ_{\parallel} and λ_{\perp} diffusivities are very useful in the interpretation of anisotropy changes — particularly when hypomyelination or reductions in axonal packing need to be differentiated from axonal injury. However, even with this additional information, several studies show reductions in both λ_{\parallel} and λ_{\perp} diffusivity and FA and axonal pathology may occur alongside myelin changes.

Second is the comparability in study methodologies. Differences, apparent at each stage of a d-MRI analysis, can impact upon the interpretation and context of results. Preterm cohorts vary widely in their degree of prematurity, local practices on the neonatal intensive care unit, frequency of lesions and macrostructural abnormalities, occurrence of comorbidities and neurodevelopmental ability. Heterogeneity is also apparent in imaging protocols and analysis methods and can influence diffusion parameters such as FA, ADC and individual eigenvalues [146].

The future of d-MRI research in preterm cohorts

Having reviewed the preterm d-MRI literature and highlighted some of its limitations, we recognise several directions and challenges for future research, and submit recommendations based on the current literature.

Due to the active and rapid development of imaging acquisition and analysis methods across centres, the impact of using specific protocols methods on diffusion parameters should be carefully considered [147, 148] as this is important for both the interpretation of results and their placement within the current literature. An evaluation of the sensitivity and specificity of analysis methods and diffusion parameters is also needed. This information is essential in determining the usefulness and contribution of d-MRI as a clinical biomarker of preterm WMI as compared to other established neuroimaging techniques. Determining the power of a given method would also improve study design by determining an adequate sample sizes in order to generate results which are likely to be more clinically meaningful. In order to better interpret diffusion findings and their relationship with neuroanatomical correlates, use of λ_{\parallel} and λ_{\perp} diffusivity is recommended wherever FA is used. Existing measures such as the ‘mode of anisotropy’ [149] may give more insight into the relationship with the

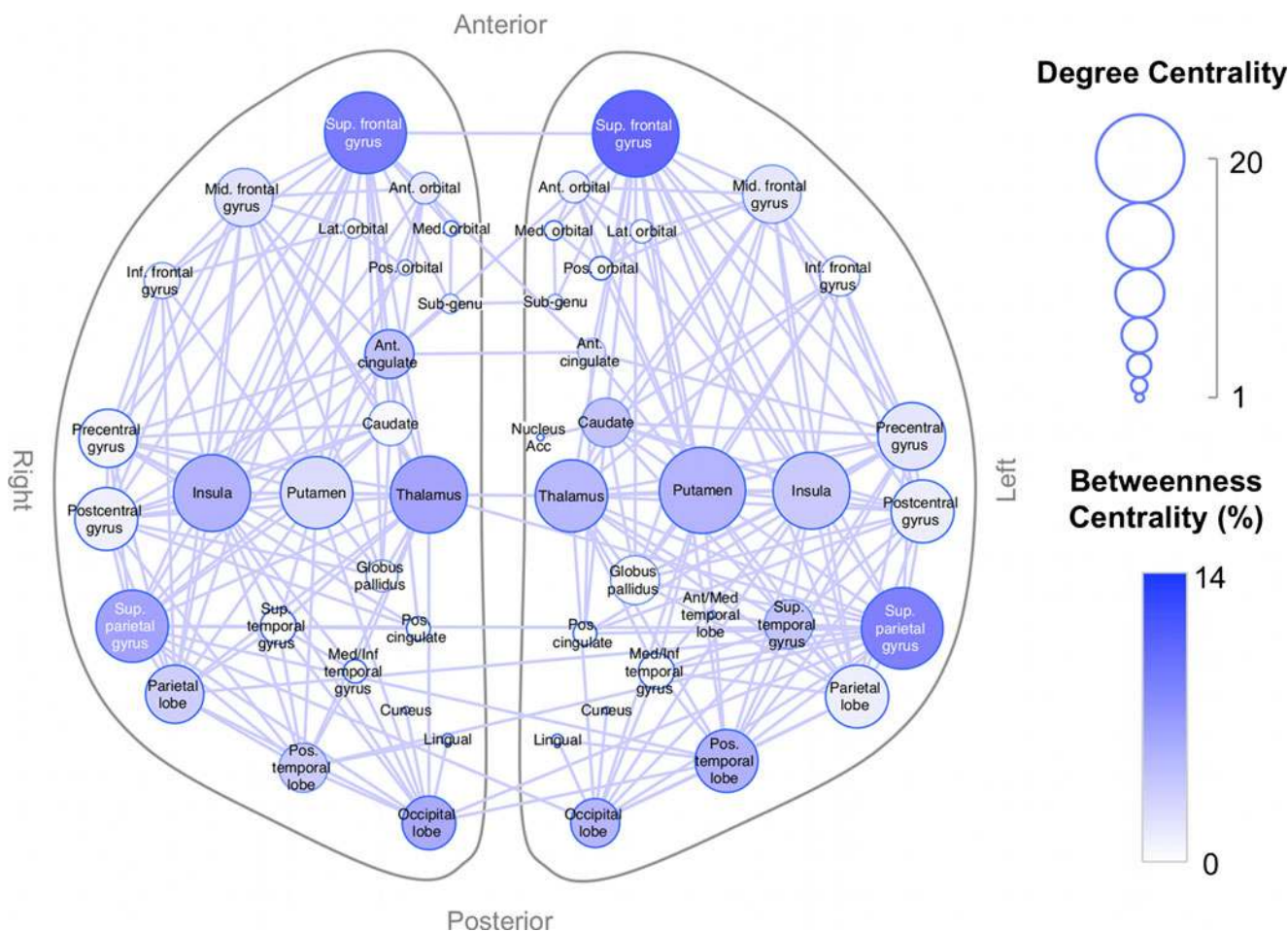


Fig. 9 Modelling of the consensus macroconnectome of preterm born children as a structural ‘network’ using graph theoretical methods. Regions of interest displayed as *circles* where the size of the circle corresponds to the degree (number of connections) and *shading* corresponds to

the local betweenness centrality (the proportion of shortest paths which pass through a region). *Sup* superior, *Inf* inferior, *Pos* posterior, *Lat* lateral, *Med* medial, *Ant* anterior. Reproduced from [92]

underlying neurobiology, as would the combined use of d-MRI with other myelination specific modalities such as Magnetization Transfer imaging [150, 151].

We anticipate improvements in acquisition schemes will increase image spatial and angular resolution to better define the complex WM architecture. Sequences with high *b* values and more gradient directions, which generate high angular resolution diffusion imaging (HARDI) MR data will be employed within clinically feasible time frames for preterm cohorts in the near future. Standard clinical d-MRI techniques currently used in preterm cohorts, such as the tensor [57] and ball and stick model [58], will be surpassed by more advanced methods, which better approximate the underlying tissue microstructure. For example, characterisation of axonal and dendritic morphology can be improved by techniques such as neurite orientation dispersion and density imaging (NODDI) [152]. Other methods such as constrained spherical deconvolution (CSD) significantly improve diffusion

tractography by providing better estimates of multiple intravoxel fibre populations [153, 154] (Fig. 8). Advances in image analysis are also anticipated. Connectome-based approaches attempt a comprehensive mapping of macrostructural connections across the whole brain [155]. Such approaches are well suited for characterising and exploring of WM connectivity in preterms without a priori assumptions of expected WM damage [92, 156, 157] (Fig. 5). Modelling of the connectome as a structural ‘network’ using graph theoretical analysis methods [158] (Fig. 9), could provide insight into complex network interactions during development and the effects of preterm WMI. Finally, an increasing data pool from both d-MRI and other quantitative MRI modalities, will drive machine learning techniques that logically combine multivariate information in order to classify subjects and identify biologically relevant patterns in complex datasets, that are associated with outcomes of interest or other clinically relevant information (i.e., genetics) [159].

Conclusion

In this article, we have presented a comprehensive review of the use of d-MRI in the study of preterm brain injury. Several limitations are recognised within the field, most notably the lack of specificity of the most commonly used diffusion-based markers for neurobiological or pathological processes, demanding careful consideration of any alterations in the context of known neurobiology. Despite these limitations, the presented studies demonstrate consistent diffusion changes indicative of WM disruption in preterm-born individuals, with poorer neurocognitive performance related to worse WM integrity in relevant functional domains. d-MRI also shows utility in the study of perinatal comorbidities and the efficacy of perinatal interventions. With advancements in image acquisition and analysis methods, d-MRI has much scope for use in the investigation of preterm WMI and as a biomarker to determine functional outcomes and evaluate clinical interventions.

Acknowledgments This work was supported by: the Medical Research Council Clinical Sciences Centre (Doctoral Studentship to AP); the NIHR Imperial College Comprehensive Biomedical Research Centre; and NIHR Comprehensive Biomedical Research Centre at Guy's and St Thomas' NHS Foundation Trust in partnership with King's College London and King's College Hospital NHS Foundation Trust.

Conflict of interest We declare that we have no conflict of interest.

References

- Petrou S, Eddama O, Mangham L (2011) A structured review of the recent literature on the economic consequences of preterm birth. *Arch Dis Child Fetal Neonatal Ed* 96:F225–F232. doi:10.1136/adc.2009.161117
- Mangham LJ, Petrou S, Doyle LW et al (2009) The cost of preterm birth throughout childhood in England and Wales. *Pediatrics* 123:e312–e327. doi:10.1542/peds.2008-1827
- Institute of Medicine (US) Committee on Understanding Premature Birth and Assuring Healthy Outcomes, Behrman RE, Butler AS (2007) *Preterm birth: causes, consequences, and prevention*. National Academies Press (US), Washington (DC)
- Saigal S, Doyle LW (2008) An overview of mortality and sequelae of preterm birth from infancy to adulthood. *Lancet* 371:261–269. doi:10.1016/S0140-6736(08)60136-1
- Kerr-Wilson CO, Mackay DF, Smith GCS, Pell JP (2011) Meta-analysis of the association between preterm delivery and intelligence. *J Public Health* 34:209–216. doi:10.1093/pubmed/fdr024
- de Kieviet JF, Zoetebier L, van Elburg RM et al (2012) Brain development of very preterm and very low-birthweight children in childhood and adolescence: a meta-analysis. *Dev Med Child Neurol* 54:313–323. doi:10.1111/j.1469-8749.2011.04216.x
- van Noort-van der Spek IL, Franken MCJP, Weisglas-Kuperus N (2012) Language functions in preterm-born children: a systematic review and meta-analysis. *Pediatrics* 129:745–754. doi:10.1542/peds.2011-1728
- Johnson S, Fawke J, Hennessy E et al (2009) Neurodevelopmental disability through 11 years of age in children born before 26 weeks of gestation. *Pediatrics* 124:e249–e257. doi:10.1542/peds.2008-3743
- Moster D, Lie RT, Markestad T (2008) Long-term medical and social consequences of preterm birth. *N Engl J Med* 359:262–273. doi:10.1056/NEJMoa0706475
- Volpe JJ (2003) Cerebral white matter injury of the premature infant—more common than you think. *Pediatrics* 112:176–180
- Volpe JJ (2008) *Neurology of the newborn*, 5th edn. Saunders, Philadelphia
- Volpe JJ (2009) Brain injury in premature infants: a complex amalgam of destructive and developmental disturbances. *Lancet Neurol* 8:110–124. doi:10.1016/S1474-4422(08)70294-1
- Deng W (2010) Neurobiology of injury to the developing brain. *Nat Rev Neurol* 6:328–336. doi:10.1038/nrneurol.2010.53
- Leviton A, Dammann O, Durum SK (2005) The adaptive immune response in neonatal cerebral white matter damage. *Ann Neurol* 58:821–828. doi:10.1002/ana.20662
- Dean JM, van de Looij Y, Sizonenko SV et al (2011) Delayed cortical impairment following lipopolysaccharide exposure in preterm fetal sheep. *Ann Neurol* 70:846–856. doi:10.1002/ana.22480
- Matute C, Alberdi E, Domercq M et al (2007) Excitotoxic damage to white matter. *J Anat* 210:693–702. doi:10.1111/j.1469-7580.2007.00733.x
- Haynes RL, Baud O, Li J et al (2006) Oxidative and nitritive injury in periventricular leukomalacia: a review. *Brain Pathol* 15:225–233. doi:10.1111/j.1750-3639.2005.tb00525.x
- Dammann O, Phillips TM, Allred EN et al (2001) Mediators of fetal inflammation in extremely low gestational age newborns. *Cytokine* 13:234–239. doi:10.1006/cyto.2000.0820
- Xanthou M, Niklas V (2012) *Inflammatory mediators in neonatal asphyxia and infection*. Neonatology. Springer, Milan, Milano, pp 853–857
- Børch K, Greisen G (1998) Blood flow distribution in the normal human preterm brain. *Pediatr Res* 43:28–33. doi:10.1203/00006450-199804001-00172
- Ballabh P, Braun A, Nedergaard M (2004) Anatomic analysis of blood vessels in germinal matrix, cerebral cortex, and white matter in developing infants. *Pediatr Res* 56:117–124. doi:10.1203/01.PDR.0000130472.30874.FF
- Soul JS, Hammer PE, Tsuji M et al (2007) Fluctuating pressure-passivity is common in the cerebral circulation of sick premature infants. *Pediatr Res* 61:467–473. doi:10.1203/pdr.0b013e31803237ff6
- Boylan GB, Young K, Panerai RB et al (2000) Dynamic cerebral autoregulation in sick newborn infants. *Pediatr Res* 48:12–17. doi:10.1203/00006450-200007000-00005
- Shankaran S, Langer JC, Kazzi SN et al (2006) Cumulative index of exposure to hypocarbia and hyperoxia as risk factors for periventricular leukomalacia in low birth weight infants. *Pediatrics* 118:1654–1659. doi:10.1542/peds.2005-2463
- Malik S, Vinukonda G, Vose LR et al (2013) Neurogenesis continues in the third trimester of pregnancy and is suppressed by premature birth. *J Neurosci* 33:411–423. doi:10.1523/JNEUROSCI.4445-12.2013
- Desilva TM, Kinney HC, Borenstein NS et al (2007) The glutamate transporter EAAT2 is transiently expressed in developing human cerebral white matter. *J Comp Neurol* 501:879–890. doi:10.1002/cne.21289
- Folkerth RD, Keefe RJ, Haynes RL et al (2006) Interferon- γ expression in periventricular leukomalacia in the human brain. *Brain Pathol* 14:265–274. doi:10.1111/j.1750-3639.2004.tb00063.x
- Billiards SS, Haynes RL, Folkerth RD et al (2006) Development of microglia in the cerebral white matter of the human fetus and infant. *J Comp Neurol* 497:199–208. doi:10.1002/cne.20991
- Verney C, Monier A, Fallet-Bianco C, Gressens P (2010) Early microglial colonization of the human forebrain and possible involvement in periventricular white-matter injury of preterm infants. *J Anat* 217:436–448. doi:10.1111/j.1469-7580.2010.01245.x

30. Drobyshevsky A, Song S-K, Gamkrelidze G et al (2005) Developmental changes in diffusion anisotropy coincide with immature oligodendrocyte progression and maturation of compound action potential. *J Neurosci* 25:5988–5997. doi:10.1523/JNEUROSCI.4983-04.2005
31. Judas M, Radoš M, Jovanov-Milosević N et al (2005) Structural, immunocytochemical, and MR imaging properties of periventricular crossroads of growing cortical pathways in preterm infants. *AJNR Am J Neuroradiol* 26:2671–2684
32. Verney C, Pogledic I, Biran V et al (2012) Microglial reaction in axonal crossroads is a hallmark of noncystic periventricular white matter injury in very preterm infants. *J Neuropathol Exp Neurol* 71:251–264. doi:10.1097/NEN.0b013e3182496429
33. Pierson CR, Folkert RD, Billiards SS et al (2007) Gray matter injury associated with periventricular leukomalacia in the premature infant. *Acta Neuropathol* 114:619–631. doi:10.1007/s00401-007-0295-5
34. Dean JM, McClendon E, Hansen K et al (2013) Prenatal cerebral ischemia disrupts MRI-defined cortical microstructure through disturbances in neuronal arborization. *Sci Transl Med* 5:168ra7. doi:10.1126/scitranslmed.3004669
35. Inder TE, Wells SJ, Mogridge NB et al (2003) Defining the nature of the cerebral abnormalities in the premature infant: a qualitative magnetic resonance imaging study. *J Pediatr* 143:171–179. doi:10.1067/S0022-3476(03)00357-3
36. Debillon T, N'Guyen S, Muet A et al (2003) Limitations of ultrasonography for diagnosing white matter damage in preterm infants. *Arch Dis Child Fetal Neonatal Ed* 88:F275–F279
37. Cheong JLY, Thompson DK, Wang HX et al (2009) Abnormal white matter signal on MR imaging is related to abnormal tissue microstructure. *Am J Neuroradiol* 30:623–628. doi:10.3174/ajnr.A1399
38. Adams E, Chau V, Poskitt KJ et al (2010) Tractography-based quantitation of corticospinal tract development in premature newborns. *J Pediatr* 156:882–888.e1. doi:10.1016/j.jpeds.2009.12.030
39. Bonifacio SL, Glass HC, Chau V et al (2010) Extreme premature birth is not associated with impaired development of brain microstructure. *J Pediatr* 157:726–732.e1. doi:10.1016/j.jpeds.2010.05.026
40. Thompson DK, Inder TE, Faggian N et al (2012) Corpus callosum alterations in very preterm infants: perinatal correlates and 2 year neurodevelopmental outcomes. *NeuroImage* 59:3571–3581. doi:10.1016/j.neuroimage.2011.11.057
41. Liu Y, Aeby A, Baleriaux D et al (2012) White matter abnormalities are related to microstructural changes in preterm neonates at term-equivalent age: a diffusion tensor imaging and probabilistic tractography study. *Am J Neuroradiol* 33:839–845. doi:10.3174/ajnr.A2872
42. van Pul C, van Kooij BJM, de Vries LS et al (2012) Quantitative fiber tracking in the corpus callosum and internal capsule reveals microstructural abnormalities in preterm infants at term-equivalent age. *Am J Neuroradiol* 33:678–684. doi:10.3174/ajnr.A2859
43. Woodward LJ, Anderson PJ, Austin NC et al (2006) Neonatal MRI to predict neurodevelopmental outcomes in preterm infants. *N Engl J Med* 355:685–694. doi:10.1056/NEJMoa053792
44. Wilke M, Krägeloh-Mann I, Holland SK (2006) Global and local development of gray and white matter volume in normal children and adolescents. *Exp Brain Res* 178:296–307. doi:10.1007/s00221-006-0732-z
45. Giedd JN, Rapoport JL (2010) Structural MRI of pediatric brain development: what have we learned and where are we going? *Neuron* 67:728–734. doi:10.1016/j.neuron.2010.08.040
46. Ment LR, Hirtz D, Hüppi PS (2009) Imaging biomarkers of outcome in the developing preterm brain. *Lancet Neurol* 8:1042–1055. doi:10.1016/S1474-4422(09)70257-1
47. Thompson DK, Inder TE, Faggian N et al (2011) Characterization of the corpus callosum in very preterm and full-term infants utilizing MRI. *NeuroImage* 55:479–490. doi:10.1016/j.neuroimage.2010.12.025
48. Nosarti C, Rushe TM, Woodruff PW et al (2004) Corpus callosum size and very preterm birth: relationship to neuropsychological outcome. *Brain* 127:2080–2089. doi:10.1093/brain/awh230
49. Narberhaus A, Segarra D, Caldú X et al (2008) Corpus callosum and prefrontal functions in adolescents with history of very preterm birth. *Neuropsychologia* 46:111–116. doi:10.1016/j.neuropsychologia.2007.08.004
50. Rakic P, Yakovlev PI (1968) Development of the corpus callosum and cavum septi in man. *J Comp Neurol* 132:45–72. doi:10.1002/cne.901320103
51. Yung A, Poon G, Qiu D, et al (2007) White matter volume and anisotropy in preterm children: a pilot study of neurocognitive correlates. *Pediatr Res*. doi:10.1203/pdr.0b013e31805365db
52. Northam GB, Liégeois F, Chong WK et al (2011) Total brain white matter is a major determinant of IQ in adolescents born preterm. *Ann Neurol* 69:702–711. doi:10.1002/ana.22263
53. Nosarti C, Giouroukou E, Healy E, et al (2008) Grey and white matter distribution in very preterm adolescents mediates neurodevelopmental outcome *Brain* 131:205–217. doi:10.1093/brain/awm282
54. Einstein A (1905) On the movement of small particles suspended in stationary liquids required by the molecular–kinetic theory of heat. *Ann Phys* 17:16
55. Stejskal TE, Tanner JE (1965) Spin diffusion measurements: spin echoes in the presence of a time-dependent field gradient. *J Chem Phys* 42:288–292
56. Moseley ME, Cohen Y, Kucharczyk J et al (1990) Diffusion-weighted MR imaging of anisotropic water diffusion in cat central nervous system. *Radiology* 176:439–445
57. Basser PJ, Pierpaoli C (1996) Microstructural and physiological features of tissues elucidated by quantitative–diffusion-tensor MRI. *J Magn Reson B* 111:209–219
58. Behrens TEJ, Woolrich MW, Jenkinson M et al (2003) Characterization and propagation of uncertainty in diffusion-weighted MR imaging. *Magn Reson Med* 50:1077–1088. doi:10.1002/mrm.10609
59. Behrens TEJ, Berg HJ, Jbabdi S et al (2007) Probabilistic diffusion tractography with multiple fibre orientations: what can we gain? *NeuroImage* 34:144–155. doi:10.1016/j.neuroimage.2006.09.018
60. Watanabe M, Sakai O, Ozonoff A et al (2013) Age-related apparent diffusion coefficient changes in the normal brain. *Radiology* 266:575–582. doi:10.1148/radiol.12112420
61. Mukherjee P, Miller JH, Shimony JS et al (2002) Diffusion-tensor MR imaging of gray and white matter development during normal human brain maturation. *AJNR Am J Neuroradiol* 23:1445–1456
62. Song S-K, Sun S-W, Ramsbottom MJ et al (2002) Demyelination revealed through MRI as increased radial (but unchanged axial) diffusion of water. *NeuroImage* 17:1429–1436
63. Takahashi M, Hackney DB, Zhang G et al (2002) Magnetic resonance microimaging of intraaxonal water diffusion in live excised lamprey spinal cord. *Proc Natl Acad Sci USA* 99:16192–16196. doi:10.1073/pnas.252249999
64. Partridge SC, Mukherjee P, Henry RG et al (2004) Diffusion tensor imaging: serial quantitation of white matter tract maturity in premature newborns. *NeuroImage* 22:1302–1314. doi:10.1016/j.neuroimage.2004.02.038
65. Gulani V, Webb AG, Duncan ID, Lauterbur PC (2001) Apparent diffusion tensor measurements in myelin-deficient rat spinal cords. *Magn Reson Med* 45:191–195. doi:10.1002/1522-2594(200102)45:2<191::AID-MRM1025>3.0.CO;2-9
66. Hüppi PS, Maier SE, Peled S et al (1998) Microstructural development of human newborn cerebral white matter assessed in vivo by diffusion tensor magnetic resonance imaging. *Pediatr Res* 44:584–590. doi:10.1203/00006450-199810000-00019
67. Schneider JFL, Il'yasov KA, Hennig J, Martin E (2004) Fast quantitative diffusion-tensor imaging of cerebral white matter from the

- neonatal period to adolescence. *Neuroradiology* 46:258–266. doi:10.1007/s00234-003-1154-2
68. Wimberger DM, Roberts TP, Barkovich AJ et al (1995) Identification of “premyelination” by diffusion-weighted MRI. *J Comput Assist Tomogr* 19:28
 69. Sun S-W, Liang H-F, Cross AH, Song S-K (2008) Evolving Wallerian degeneration after transient retinal ischemia in mice characterized by diffusion tensor imaging. *NeuroImage* 40:1–10. doi:10.1016/j.neuroimage.2007.11.049
 70. Wu Q, Butzkueven H, Gresle M et al (2007) MR diffusion changes correlate with ultra-structurally defined axonal degeneration in murine optic nerve. *NeuroImage* 37:1138–1147. doi:10.1016/j.neuroimage.2007.06.029
 71. Bonekamp D, NAGAE LM, Degaonkar M et al (2007) Diffusion tensor imaging in children and adolescents: reproducibility, hemispheric, and age-related differences. *NeuroImage* 34:733–742. doi:10.1016/j.neuroimage.2006.09.020
 72. Bisdas S, Bohning DE, Besenski N et al (2008) Reproducibility, interrater agreement, and age-related changes of fractional anisotropy measures at 3T in healthy subjects: effect of the applied *b*-value. *Am J Neuroradiol* 29:1128–1133. doi:10.3174/ajnr.A1044
 73. Lepomäki VK, Paavilainen TP, et al (2011) Fractional anisotropy and mean diffusivity parameters of the brain white matter tracts in preterm infants: reproducibility of region-of-interest measurements. *Pediatr Radiol*. doi: 10.1007/s00247-011-2234-9
 74. Cabezas M, Oliver A, Lladó X et al (2011) A review of atlas-based segmentation for magnetic resonance brain images. *Comput Methods Prog Biomed* 104:e158–e177. doi:10.1016/j.cmpb.2011.07.015
 75. Ashburner J, Friston KJ (2000) Voxel-based morphometry—the methods. *NeuroImage* 11:805–821. doi:10.1006/nimg.2000.0582
 76. Ashburner J, Friston KJ (2005) Unified segmentation. *NeuroImage* 26:839–851. doi:10.1016/j.neuroimage.2005.02.018
 77. Smith SM, Jenkinson M, Johansen-Berg H et al (2006) Tract-based spatial statistics: voxelwise analysis of multi-subject diffusion data. *NeuroImage* 31:1487–1505. doi:10.1016/j.neuroimage.2006.02.024
 78. Conturo TE, Lori NF, Cull TS et al (1999) Tracking neuronal fiber pathways in the living human brain. *Proc Natl Acad Sci USA* 96:10422–10427
 79. Catani M, Howard RJ, Pajevic S, Jones DK (2002) Virtual in vivo interactive dissection of white matter fasciculi in the human brain. *NeuroImage* 17:77–94
 80. Yakovlev PI, Lecours A-R (1967) The myelogenetic cycles of regional maturation of the brain. In: Minowski A (ed) *Regional development of the brain in early life*, Blackwell, Oxford, pp 3–70
 81. Kinney HC, Brody BA, Kloman AS, Gilles FH (1988) Sequence of central nervous system myelination in human infancy: II. Patterns of myelination in autopsied infants. *J Neuropathol Exp Neurol* 47:217
 82. Aeby A, Liu Y, De Tiège X et al (2009) Maturation of thalamic radiations between 34 and 41 weeks' gestation: a combined voxel-based study and probabilistic tractography with diffusion tensor imaging. *Am J Neuroradiol* 30:1780–1786. doi:10.3174/ajnr.A1660
 83. Anjari M, Srinivasan L, Allsop JM et al (2007) Diffusion tensor imaging with tract-based spatial statistics reveals local white matter abnormalities in preterm infants. *NeuroImage* 35:1021–1027. doi:10.1016/j.neuroimage.2007.01.035
 84. Rose SE, Hatzigeorgiou X, Strudwick MW et al (2008) Altered white matter diffusion anisotropy in normal and preterm infants at term-equivalent age. *Magn Reson Med* 60:761–767. doi:10.1002/mrm.21689
 85. Hasegawa T, Yamada K, Morimoto M et al (2011) Development of corpus callosum in preterm infants is affected by the prematurity: in vivo assessment of diffusion tensor imaging at term-equivalent age. *Pediatr Res* 69:249–254. doi:10.1203/PDR.0b013e3182084e54
 86. Dudink J, Lequin M, Pul C et al (2007) Fractional anisotropy in white matter tracts of very-low-birth-weight infants. *Pediatr Radiol* 37:1216–1223. doi:10.1007/s00247-007-0626-7
 87. Ball G, Boardman JP, Rueckert D et al (2012) The effect of preterm birth on thalamic and cortical development. *Cereb Cortex* 22:1016–1024. doi:10.1093/cercor/bhr176
 88. Miller SP, Vigneron DB, Henry RG et al (2002) Serial quantitative diffusion tensor MRI of the premature brain: development in newborns with and without injury. *J Magn Reson Imaging* 16:621–632. doi:10.1002/jmri.10205
 89. Lee AY, Jang SH, Lee E, et al (2012) Radiologic differences in white matter maturation between preterm and full-term infants: TBSS study. *Pediatr Radiol*. doi: 10.1007/s00247-012-2545-5
 90. Jo HM, Cho HK, Jang SH, et al (2012) A comparison of microstructural maturational changes of the corpus callosum in preterm and full-term children: a diffusion tensor imaging study. *Neuroradiology*. doi: 10.1007/s00234-012-1042-8
 91. Wang S, Fan G, Xu K, Wang C (2012) Potential of diffusion tensor MR imaging in the assessment of cognitive impairments in children with periventricular leukomalacia born preterm. *Eur J Radiol*. doi: 10.1016/j.ejrad.2012.06.032
 92. Pandit AS, Robinson E, Aljabar P, et al. (2013) Whole-brain mapping of structural connectivity in infants reveals altered connection strength associated with growth and Preterm birth. *Cereb Cortex*. doi: 10.1093/cercor/bht086
 93. Vangberg TR, Skranes J, Dale AM et al (2006) Changes in white matter diffusion anisotropy in adolescents born prematurely. *NeuroImage* 32:1538–1548. doi:10.1016/j.neuroimage.2006.04.230
 94. Skranes J, Vangberg TR, Kulseng S et al (2007) Clinical findings and white matter abnormalities seen on diffusion tensor imaging in adolescents with very low birth weight. *Brain* 130:654–666. doi:10.1093/brain/awm001
 95. Constable RT, Ment LR, Vohr BR et al (2008) Prematurely born children demonstrate white matter microstructural differences at 12 years of age, relative to term control subjects: an investigation of group and gender effects. *Pediatrics* 121:306–316. doi:10.1542/peds.2007-0414
 96. Mullen KM, Vohr BR, Katz KH et al (2011) Preterm birth results in alterations in neural connectivity at age 16 years. *NeuroImage* 54:2563–2570. doi:10.1016/j.neuroimage.2010.11.019
 97. Feldman HM, Lee ES, Loe IM et al (2012) White matter microstructure on diffusion tensor imaging is associated with conventional magnetic resonance imaging findings and cognitive function in adolescents born preterm. *Dev Med Child Neurol* 54:809–814. doi:10.1111/j.1469-8749.2012.04378.x
 98. Kontis D, Catani M, Cuddy M et al (2009) Diffusion tensor MRI of the corpus callosum and cognitive function in adults born preterm. *Neuroreport* 20:424–428. doi:10.1097/WNR.0b013e328325a8f9
 99. Allin MPG, Kontis D, Walshe M et al (2011) White matter and cognition in adults who were born preterm. *PLoS One* 6:e24525. doi:10.1371/journal.pone.0024525
 100. Eikenes L, Løhaugen GC, Brubakk A-M et al (2011) Young adults born preterm with very low birth weight demonstrate widespread white matter alterations on brain DTI. *NeuroImage* 54:1774–1785. doi:10.1016/j.neuroimage.2010.10.037
 101. Johansen-Berg H (2010) Behavioural relevance of variation in white matter microstructure. *Curr Opin Neurol* 1. doi: 10.1097/WCO.0b013e32833b7631
 102. Bassi L, Ricci D, Volzone A et al (2008) Probabilistic diffusion tractography of the optic radiations and visual function in preterm infants at term equivalent age. *Brain* 131(Pt 2):573–582. doi:10.1093/brain/awm327
 103. Berman JI, Glass HC, Miller SP et al (2008) Quantitative fiber tracking analysis of the optic radiation correlated with visual performance in premature newborns. *Am J Neuroradiol* 30:120–124. doi:10.3174/ajnr.A1304
 104. Glass HC, Berman JI, Norcia AM et al (2010) quantitative fiber tracking of the optic radiation is correlated with visual-evoked

- potential amplitude in preterm infants. *Am J Neuroradiol* 31:1424–1429. doi:10.3174/ajnr.A2110
105. Groppo M, Ricci D, Bassi L, et al (2012) Development of the optic radiations and visual function after premature birth. *Cortex* 1–35. doi: 10.1016/j.cortex.2012.02.008
 106. Lindqvist S, Skranes J, Eikenes L et al (2011) Visual function and white matter microstructure in very-low-birth-weight (VLBW) adolescents—a DTI study. *Vis Res* 51:2063–2070. doi:10.1016/j.visres.2011.08.002
 107. Reiman M, Parkkola R, Johansson R et al (2009) Diffusion tensor imaging of the inferior colliculus and brainstem auditory-evoked potentials in preterm infants. *Pediatr Radiol* 39:804–809. doi:10.1007/s00247-009-1278-6
 108. Mesulam M (2000) Brain, mind, and the evolution of connectivity. *Brain Cogn* 42:4–6. doi:10.1006/brcg.1999.1145
 109. Choi YY, Shamosh NA, Cho SH et al (2008) Multiple bases of human intelligence revealed by cortical thickness and neural activation. *J Neurosci* 28:10323–10329. doi:10.1523/JNEUROSCI.3259-08.2008
 110. Mesulam M (2012) The evolving landscape of human cortical connectivity: facts and inferences. *NeuroImage* 62:2182–2189. doi:10.1016/j.neuroimage.2011.12.033
 111. Khong P, Qiu D, Yung A, Poon G (2006) Regional white matter anisotropy and general intelligence in preterm born children: a voxelwise analysis. *Proceedings of the International Society for Magnetic Resonance in medicine*: 3407
 112. Counsell SJ, Edwards AD, Chew ATM et al (2008) Specific relations between neurodevelopmental abilities and white matter microstructure in children born preterm. *Brain* 131:3201–3208. doi:10.1093/brain/awn268
 113. van Kooij BJM, de Vries LS, Ball G, et al. (2011) Neonatal tract-based spatial statistics findings and outcome in preterm Infants. *Am J Neuroradiol*. doi: 10.3174/ajnr.A2723
 114. Skranes J, Løhaugen GC, Martinussen M et al (2009) White matter abnormalities and executive function in children with very low birth weight. *Neuroreport* 20:263–266. doi:10.1097/WNR.0b013e32832027fe
 115. Johnson MH, de Haan M (2010) *Developmental cognitive neuroscience*, 3rd edition. Wiley-Blackwell, Oxford, pp 1–316
 116. Hickok G, Poeppel D (2007) The cortical organization of speech processing. *Nat Rev Neurosci* 8:393–402. doi:10.1038/nrn2113
 117. Friederici AD (2009) Pathways to language: fiber tracts in the human brain. *Trends Cogn Sci* 13:175–181. doi:10.1016/j.tics.2009.01.001
 118. Friederici AD, Alter K (2004) Lateralization of auditory language functions: a dynamic dual pathway model. *Brain Lang* 89:267–276. doi:10.1016/S0093-934X(03)00351-1
 119. Catani M, Allin MPG, Husain M et al (2007) Symmetries in human brain language pathways correlate with verbal recall. *Proc Natl Acad Sci USA* 104:17163–17168. doi:10.1073/pnas.0702116104
 120. Lebel C, Beaulieu C (2009) Lateralization of the arcuate fasciculus from childhood to adulthood and its relation to cognitive abilities in children. *Hum Brain Mapp* 30:3563–3573. doi:10.1002/hbm.20779
 121. Feldman HM, Lee ES, Yeatman JD, Yeom KW (2012) Language and reading skills in school-aged children and adolescents born preterm are associated with white matter properties on diffusion tensor imaging. *Neuropsychologia* 50:3348–3362. doi:10.1016/j.neuropsychologia.2012.10.014
 122. Northam GB, Liegeois F, Tournier JD et al (2012) Interhemispheric temporal lobe connectivity predicts language impairment in adolescents born preterm. *Brain* 135:3781–3798. doi:10.1093/brain/aws276
 123. Williams J, Lee KJ, Anderson PJ (2010) Prevalence of motor-skill impairment in preterm children who do not develop cerebral palsy: a systematic review. *Dev Med Child Neurol* 52:232–237. doi:10.1111/j.1469-8749.2009.03544.x
 124. Rose J, Butler EE, Lamont LE et al (2009) Neonatal brain structure on MRI and diffusion tensor imaging, sex, and neurodevelopment in very-low-birthweight preterm children. *Dev Med Child Neurol* 51:526–535. doi:10.1111/j.1469-8749.2008.03231.x
 125. Northam GB, Liégeois F, Chong WK et al (2012) Speech and oromotor outcome in adolescents born preterm: relationship to motor tract integrity. *J Pediatr* 160:402–408.e1. doi:10.1016/j.jpeds.2011.08.055
 126. Pharoah PO, Cooke T, Cooke RW, Rosenbloom L (1990) Birthweight specific trends in cerebral palsy. *Arch Dis Child* 65:602–606
 127. Bax M, Goldstein M, Rosenbaum P et al (2005) Proposed definition and classification of cerebral palsy, April 2005. *Dev Med Child Neurol* 47:571–576. doi:10.1017/S001216220500112X
 128. Scheck SM, Boyd RN, Rose SE (2012) New insights into the pathology of white matter tracts in cerebral palsy from diffusion magnetic resonance imaging: a systematic review. *Dev Med Child Neurol* 54:684–696. doi:10.1111/j.1469-8749.2012.04332.x
 129. Rutherford MA, Supramaniam V, Ederies A et al (2010) Magnetic resonance imaging of white matter diseases of prematurity. *Neuroradiology* 52:505–521. doi:10.1007/s00234-010-0700-y
 130. Johnson S, Marlow N (2011) Preterm birth and childhood psychiatric disorders. *Pediatr Res* 69:11R–18R. doi:10.1203/PDR.0b013e318212faa0
 131. Sansavini A, Guarini A, Caselli MC (2011) Preterm birth: neuropsychological profiles and atypical developmental pathways. *Dev Disabil Res Revs* 17:102–113. doi:10.1002/ddrr.1105
 132. Bhutta AT, Cleves MA, Casey PH et al (2002) Cognitive and behavioral outcomes of school-aged children who were born preterm: a meta-analysis. *JAMA* 288:728–737
 133. Aarnoudse-Moens CSH, Weisglas-Kuperus N, van Goudoever JB, Oosterlaan J (2009) Meta-analysis of neurobehavioral outcomes in very preterm and/or very low birth weight children. *Pediatrics* 124:717–728. doi:10.1542/peds.2008-2816
 134. Rogers CE, Anderson PJ, Thompson DK et al (2012) Regional cerebral development at term relates to school-age social-emotional development in very preterm children. *J Am Acad Child Adolesc Psychiatry* 51:181–191. doi:10.1016/j.jaac.2011.11.009
 135. Nagy Z, Westerberg H, Skare S et al (2003) Preterm children have disturbances of white matter at 11 years of age as shown by diffusion tensor imaging. *Pediatr Res* 54:672–679. doi:10.1203/01.PDR.0000084083.71422.16
 136. Stoll BJ, Hansen NI, Adams-Chapman I et al (2004) Neurodevelopmental and growth impairment among extremely low-birth-weight infants with neonatal infection. *JAMA* 292:2357–2365
 137. Chau V, Brant R, Poskitt KJ et al (2012) Postnatal infection is associated with widespread abnormalities of brain development in premature newborns. *Pediatr Res* 71:274–279. doi:10.1038/pr.2011.40
 138. Chau V, Poskitt KJ, McFadden D et al (2009) Effect of chorioamnionitis on brain development and injury in premature newborns. *Ann Neurol* 66:127–129. doi:10.1002/ana.21761
 139. Hemels MA, Nijman J, Leemans A et al (2012) Cerebral white matter and neurodevelopment of preterm infants after coagulase-negative staphylococcal sepsis. *Pediatr Crit Care Med* 13:678–684. doi:10.1097/PCC.0b013e3182455778
 140. Hibbard JU, Wilkins I, Sun L et al (2010) Respiratory morbidity in late preterm births. *JAMA* 304:419–425
 141. Anjari M, Counsell SJ, Srinivasan L et al (2009) The association of lung disease with cerebral white matter abnormalities in preterm infants. *Pediatrics* 124:268–276. doi:10.1542/peds.2008-1294
 142. Ball G, Counsell SJ, Anjari M et al (2010) An optimised tract-based spatial statistics protocol for neonates: applications to prematurity and chronic lung disease. *NeuroImage* 53:94–102. doi:10.1016/j.neuroimage.2010.05.055

143. Doyle LW, Cheong J, Hunt RW et al (2010) Caffeine and brain development in very preterm infants. *Ann Neurol* 68:734–742. doi:10.1002/ana.22098
144. Milgrom J, Newnham C, Anderson PJ et al (2010) Early sensitivity training for parents of preterm infants: impact on the developing brain. *Pediatr Res* 67:330–335. doi:10.1203/PDR.0b013e3181cb8e2f
145. Als H, Duffy FH, McAnulty GB et al (2004) Early experience alters brain function and structure. *Pediatrics* 113:846–857
146. Ni H, Kavcic V, Zhu T et al (2006) Effects of number of diffusion gradient directions on derived diffusion tensor imaging indices in human brain. *AJNR Am J Neuroradiol* 27:1776–1781
147. Magnotta VA, Matsui JT, Liu D et al (2012) Multicenter reliability of diffusion tensor imaging. *Brain Connect* 2:345–355. doi:10.1089/brain.2012.0112
148. Fox RJ, Sakaie K, Lee JC et al (2012) A validation study of multicenter diffusion tensor imaging: reliability of fractional anisotropy and diffusivity values. *Am J Neuroradiol* 33:695–700. doi:10.3174/ajnr.A2844
149. Ennis DB, Kindlmann G (2005) Orthogonal tensor invariants and the analysis of diffusion tensor magnetic resonance images. *Magn Reson Med* 55:136–146. doi:10.1002/mrm.20741
150. Engelbrecht V, Scherer A, Rassek M et al (2002) Diffusion-weighted MR imaging in the brain in children: findings in the normal brain and in the brain with white matter diseases. *Radiology* 222:410–418. doi:10.1148/radiol.2222010492
151. Mädler B, Drabycz SA, Kolind SH et al (2008) Is diffusion anisotropy an accurate monitor of myelination? *Magn Reson Imaging* 26:874–888. doi:10.1016/j.mri.2008.01.047
152. Zhang H, Schneider T, Wheeler-Kingshott CA, Alexander DC (2012) NODDI: practical in vivo neurite orientation dispersion and density imaging of the human brain. *NeuroImage* 61:1000–1016. doi:10.1016/j.neuroimage.2012.03.072
153. Tournier J-D, Calamante F, Connelly A (2007) Robust determination of the fibre orientation distribution in diffusion MRI: non-negativity constrained super-resolved spherical deconvolution. *NeuroImage* 35:1459–1472. doi:10.1016/j.neuroimage.2007.02.016
154. Jeurissen B, Leemans A, Jones DK et al (2011) Probabilistic fiber tracking using the residual bootstrap with constrained spherical deconvolution. *Hum Brain Mapp* 32:461–479. doi:10.1002/hbm.21032
155. Sporns O, Tononi G, Kötter R (2005) The Human Connectome: a structural description of the human brain. *PLoS Comput Biol* 1:e42. doi:10.1371/journal.pcbi.0010042
156. Ball G, Boardman JP, Aljabar P, et al (2012) The influence of preterm birth on the developing thalamocortical connectome. *Cortex*. 2013 Jun;49(6):1711–1721. doi: 10.1016/j.cortex.2012.07.006. Epub 2012 Aug 9
157. Tymofiyeva O, Hess CP, Ziv E et al (2012) Towards the “baby connectome”: mapping the structural connectivity of the newborn brain. *PLoS One* 7:e31029. doi:10.1371/journal.pone.0031029
158. Bullmore E, Sporns O (2009) Complex brain networks: graph theoretical analysis of structural and functional systems. *Nat Rev Neurosci* 10:186–198. doi:10.1038/nrn2575
159. Wolz R, Aljabar P, Hajnal JV, et al. (2012) Medical image analysis. *Med Image Anal* 1–12. doi: 10.1016/j.media.2011.12.003

Review criteria

References for this review were identified through searches of PubMed and Google Scholar before March 2013. Combinations of the following search terms were used: “MRI”, “magnetic resonance imaging”, “diffusion weighted”, “diffusion MR*”, “DTI”, “diffusion tensor*”, “tractography”, “structural connectivity”, “white matter”, “WM”, “preterm”, “prematu*”, “neonate”, “infant”, “child”, “adolescent”, “adult”. Although birth weight may not be an exact proxy for the degree of prematurity, given its frequent use in the literature we have also used search terms: “low birth weight”, “LBW”, “VLBW”. Only articles written in English were included. Studies were critically appraised and those which were felt to have most relevance to the topic were selected.